Advances in Membrane, Dialyzer Design and Related Monitoring Technology for Hemodiafiltration: Translating Bench Side Innovations to Bedside Applications

Alfred Josef Gagel *, Gerhard Wiesen, Stefano Stuard, Bernard Canaud

Posted Date: 4 February 2026

doi: 10.20944/preprints202602.0325.v1

Keywords: hemodiafiltration; dialysis membrane; convective volume; synthetic polymers; uremic toxin clearance; ultrafiltration; albumin loss; kidney replacement therapy

 doi:10.20944/preprints202602.0325.v1

Article

Advances in Membrane, Dialyzer Design and Related Monitoring Technology for Hemodiafiltration: Translating Bench Side Innovations to Bedside Applications

Alfred Josef Gagel [1,*], Gerhard Wiesen [1], Stefano Stuard [2] and Bernard Canaud [3]

[1] Global Research and Development, Fresenius Medical Care Deutschland GmbH, Bad Homburg, Germany
[2] Global Medical Office, Fresenius Medical Care, 26020 Palazzo Pignano, Italy
[3] Montpellier University, School of Medicine & AIDER-Santé, Foundation Ch Mion, Montpellier, France
* alfred.gagel@freseniusmedicalcare.com

Abstract

Background: Online hemodiafiltration (HDF) is currently the most advanced kidney replacement therapy that combines diffusive and convective solute removal to clear uremic toxins, particularly larger molecular compounds. Effective HDF therapy is contingent on achieving a high total convective volume, impacting patient survival. **Objectives**: To explore advancements in dialysis membrane materials, dialyzer design and related monitoring technology that enhance HDF performance, particularly in removing middle and larger uremic toxins, and to examine the challenges related to membrane hemocompatibility, permeability, and optimizing clinical performances. **Methods**: This review synthesizes findings on materials used in dialysis membranes, advanced technology to spin fibers and dialyzer design, and related monitoring technology emphasizing their effects on hydraulic permeability, solute clearance and hemocompatibility. It also links them to clinical studies that have proved the beneficial impact of convective volume on patient outcomes. **Results**: Synthetic polymer membranes, such as polysulfone and polyethersulfone together with advances in hollow-fiber spinning technology, have improved the middle molecules clearance through optimized pore sizes and higher ultrafiltration coefficients. When combined with advanced hemodiafiltration machines designed to optimize convective volume and dialysate use, that maximizes convection efficiency **while maintaining patient safety** comparable to conventional hemodialysis. The development of super-high-flux membranes in a revisited internal filtration approach, known as expanded hemodialysis enhances toxin removal but can lead to albumin loss and inflammatory responses if ultrapure dialysate is not provided. Achieving the right balance in membrane design is essential to delivering efficient and high-volume HDF while minimizing potential adverse effects. **Conclusion**: Advanced dialysis membranes and HDF monitoring technologies significantly enhance the efficacy of HDF by enabling efficient removal of middle and large uremic toxins. Continued innovation in materials science and dialyzer membrane architecture is essential to further optimize patient outcomes and to consolidate HDF as a mainstream renal replacement therapy.

Keywords: hemodiafiltration; dialysis membrane; convective volume; synthetic polymers; uremic toxin clearance; ultrafiltration; albumin loss; kidney replacement therapy

1. Introduction

Online hemodiafiltration (HDF) represents the most advanced form of kidney replacement therapy, integrating both diffusive and convective solute transport to effectively remove uremic toxins, especially middle and large-molecular-weight compounds that are challenging to clear with

 doi:10.20944/preprints202602.0325.v1

conventional hemodialysis [1,47] and it improves the elimination of PBUTs like indoxyl sulfate and p-cresyl sulfate [52–54]. The efficacy and clinical benefits of HDF are closely tied to the total convective volume or ultrafiltration delivered per session, a key indicator of the removal of these larger solutes [2–5]. Solute clearance in HDF relies on several factors: the filtration fraction (the ratio of ultrafiltered plasma water flow to blood flow rate), the blood flow rate, the sieving capacity of the filter, which is strongly influenced by blood flow rates, and the overall treatment duration [2,3]. As demonstrated by the recent CONVINCE study, achieving a threshold convective volume of 23 liters, in addition to the net ultrafiltration volume, was essential to reducing all-cause mortality by 23% [6]. Further confirmed by an updated individual patient data meta-analysis involving more 4000 patients, hemodiafiltration is associated with a reduction of relative risk of death both in all-cause and cardiovascular origins in almost linear fashion with convective volume as more is better [7,8,49,50]. The clinical and biological benefits of high volume hemodiafiltration in kidney care have been clearly highlighted in a recent comprehensive review [57].

Central to this process is the hemodialyzer membrane, which acts as a selective barrier, allowing uremic toxins to pass through while retaining essential proteins including albumin [9–11]. The effectiveness of HDF also depends on patient-specific blood factors (e.g., hematocrit, protein concentration), transmembrane pressure management (either manual or automated), and operational conditions such as blood flow rate, substitution modality (post- versus pre-dilution), anticoagulation, and net ultrafiltration [3,12]. Early dialysis membranes, composed of cellulose, were limited in their capacity to clear larger molecules and frequently triggered inflammatory responses due to poor hemocompatibility and low hydraulic permeability [11]. Advances in materials and fiber spinning technology have led to the development of synthetic polymer membranes, such as polysulfone, polyethersulfone, and polyacrylonitrile, with fibers that have finely tuned pore size distributions, offering improved clearance and a better hemocompatibility profile [13,14]. The design and quality-controlled manufacturing of these membranes are critical to achieve an optimal balance between effective toxin removal and minimal loss of albumin. Middle Cut Off (MCO) and super-high-flux membranes with larger pores enhance middle-molecule clearance in hemodialysis but may increase the risk of albumin loss when high ultrafiltration flow is imposed [15–17]. Moreover, contact between blood and the membrane triggers hemoincompatibility reactions, including the activation of clotting, complement, and bradykinin cascades, as well as circulating cell stimulation, potentially leading to systemic inflammatory responses and contributing to organ damage [18]. The formation of a secondary protein layer on the membrane further alters filtration dynamics, affecting clearance efficiency and increasing transmembrane pressures [1]. Automated management of these variables through advanced, proprietary features of modern hemodiafiltration machines is essential for maintaining patient safety and ensuring treatment efficacy. Additional challenges, such as maintaining stable transmembrane pressures, preventing back-filtration, and controlling electrolyte balance, can complicate high-volume HDF, making membrane selection and the interaction between dialyzer and HDF machine crucial. While these factors are all essential, this manuscript will focus specifically on the role of the dialysis membrane.

Therefore, the ideal membrane must meet strict criteria for permeability, hemocompatibility, and stability under high convective volumes, establishing it as a key component in advancing HDF as mainstream therapeutic option.

2. Hemodialysis Membrane and Solute Transfer

2.1. Membrane Material

In the early years of dialysis, membranes were primarily produced from regenerated cellulose. The characteristics of the cellulose-based membrane range was a comparably low hydraulic permeability or ultrafiltration flow rate for plasma water [9,11]. Dialysis machines could regulate the weight loss of patients simply by means of transmembrane pressure control. Symmetric membrane walls with a thickness of 6-8 μm entailed short diffusive distances and proved to be efficient in

 doi:10.20944/preprints202602.0325.v1

diffusive clearance. While clearances of small molecules as urea and creatinine were satisfying, middle-molecular substances as e.g. ß2-microglobulin could not be removed in an adequate manner.

With the appearance of membranes spun from synthetic materials, different elimination characteristics were achieved – or were the consequence of production processes and were much harder to control. Pore size spectra covered a much higher range and filtration flow rates were much higher [19]. As the flow resistance of a membrane pore decreases with the power of four (law of Hagen-Poiseuille), doubling the pore diameter meant a sixteen-fold higher filtration rate. Care had to be given to the aspect of potentially excessive plasma water loss during the dialysis treatment which was leading to the development of dialysis machines with dialysate volume balancing systems and a tight control of ultrafiltration volumes. The ultrafiltration capacity of the membranes beyond the volume needed for fluid status control of dialysis patients has offered the prospect of additional filtration volumes in the hemodiafiltration modality.

Various polymers have been used to produce dialysis membranes. The first materials successfully used were acrylonitrile (Rhone Poulenc), polyacrylonitrile (Asahi), polysulfone (Amicon), polyamide (Gambro) and polymethylmethacrylate (PMMA, Teijin). However, membrane characteristics cannot be derived from the polymer alone since membrane production including sterilization has a significant effect on the final membrane morphology and pore size distribution [20]. Furthermore, optimal hydrophilicity distribution is often reached by adding polar polymers [21,22]. However, suitability depends as well on transmembrane resistance during the treatment, which seems to be more critical in PMMA and triacetate membranes [23].

2.2. Membrane Hemocompatibility

A basic prerequisite of dialysis membranes is the hemocompatibility of the membrane material as well as the potting material separating the blood from the dialysate compartment and the materials of the dialyzer housing. Low coagulation activation and low stimulation of active immune response (e.g., complement, phase contact and bradykinin systems) are key for the use in chronic kidney replacement therapy [18].

The development of new polymers compounds and membrane surface treatments has considerably reduced blood-membrane interaction reactions. In addition, modern automated production processes and production monitoring by improved laboratory equipment have continuously enhanced dialyzer quality. The migration of chemicals and release of particles have been reduced to extremely low level, further minimizing immune system stimulation.

Considering the potential risks posed by dialysis fluid contaminants due to back-diffusion and back-filtration, synthetic high flux membranes achieve excellent retention of dialysate contaminants (e.g. bacteria, virus, endotoxins, by-products and organic/inorganic particles). This safety barrier of high flux dialyzers, combined with point-of-use sterilizing ultrafilters in the dialysis machine's hydraulic system for the preparation of ultrapure dialysis fluid or online preparation of sterile substitution fluid, minimizes inflammatory and immune system responses caused by dialysis fluid contaminants.

MCO membranes have larger pores than high-flux membranes, which facilitate through internal filtration phenomena better removal of larger middle molecules by hemodialysis. But on the other side, the more open structure of the membrane could enhance the transfer of pyrogens like endotoxins and other bacterial contaminants into patient's blood, which can be present in non-pyrogen free dialysis fluid. They are not suitable for HDF treatments because they exhibit significantly higher permeability to albumin and plasma proteins compared with standard high-flux membranes when exposed to high transmembrane pressure, resulting in clinically unacceptable protein losses.

2.3. Membrane Permeability: Pore Size Selectivity and Distribution

The total filtration flow rate across the dialyzer membrane normalized for the applied transmembrane pressure gives the ultrafiltration coefficient (K_{UF}). It can be taken to categorize

 doi:10.20944/preprints202602.0325.v1

membranes of low, medium or high hydraulic permeability of water. However, the more relevant characteristic of low and middle molecular elimination performance cannot be derived from the KUF.

The steepness of the cut-off curve can be utilized as an essential performance parameter for the efficacy of high-flux membranes regarding the removal capacity of middle molecules. It is based on the sieving characteristic of the membrane and is quantified by the sieving coefficient S, which is defined as the ratio of the solute concentration in filtrate C_f and that in feed solution C_{in}:

$$S = \frac{C_f}{C_{in}} \qquad (2.1)$$

Size exclusion of solutes by the sieving characteristic of dialysis membranes is depicted in Figure 2.6.

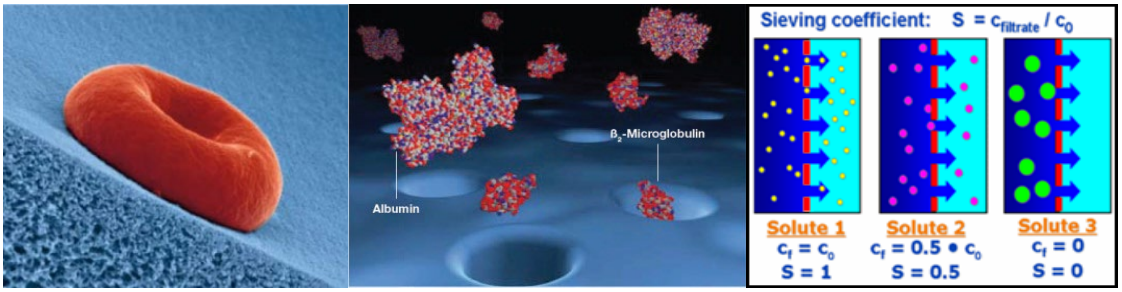

Figure 2.6. Size exclusion and sieving coefficient of dialysis membranes.

Sieving coefficients for the spectrum of relevant molecular substances gives deeper insight into the elimination capacity for uremic solutes. Typically shown in semi-logarithmic graphs the sieving coefficients of high flux membranes stay at a value of 1, or a probability of 100%, to cross the membrane for substances in the low molecular range. The molecular weight of proteins, whose sizes exceed the smallest pore sizes, mark the onset the cut-off region onset (MWRO) at sieving coefficient S = 90%. It starts in modern high-flux dialyzers at molecular masses of about 10 kDa or of ß2-microglobulin (ß2m, 11.8kDa). The upper end of the cut-off region is indicated by the molecular weight of proteins, whose sizes exceed the biggest pores of the membrane (MWCO) at sieving coefficient at S = 10%. [31]

A steeper sieving curve (SC) and a narrower cut-off region is achieved with a tighter pore size distribution and can be characterized by the molecular weight ratio of MWRO and MWCO:

$$SC_{steepness} = \frac{MWRO\ (S{=}90\%)}{MWCO\ (S{=}10\%)} \qquad (2.2)$$

Beyond 60.000 Da, typically the size of albumin (HSA, 67 kDa), the sieving coefficients reach values below one percent to limit the loss of albumin and other large proteins, especially under hemodiafiltration conditions. The sieving characteristic is adjusted to that of healthy kidneys in this molecular range.

In case of low flux membranes, the molecular weight cut-off value (90% retention of substances with the respective weight) is much smaller, i.e. only low molecular substances can be effectively eliminated due to the small pore sizes (see Figure 2.1).

 doi:10.20944/preprints202602.0325.v1

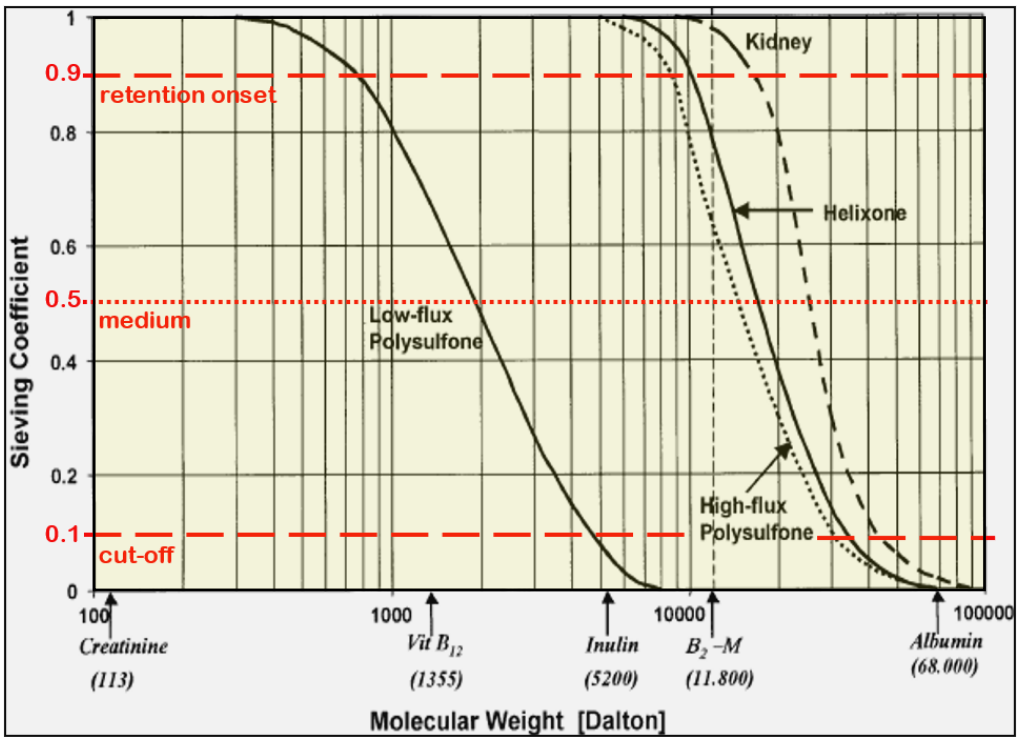

Figure 2.1. Sieving coefficient of low- and high-flux polysulfone membranes and of kidney as function of the molecular weight.

In order to approach the entire sieving characteristic of the kidney, the sieving curves of the membranes would have to be much steeper. However, nowadays membranes are limited by technical constraints in serial production.

The formation of the membrane by phase inversion is a stochastic process, which generates broader pore size distributions with larger mean pore sizes. Consequently, MCO membranes have usually broader pore size distributions than high-flux dialyzers and have less steep cut-off sieving curves, and not the other way round as often depicted.

2.4. Solute Membrane Transfer Mechanisms in HDF

2.4.1. Solute Transfer by Diffusion and by Convection

Diffusion is the movement of solutes from a region with higher concentration to a region with lower concentration [24]. It is driven by a concentration gradient dC/dx. The motion is powered by the thermal energy of the solution, and the speed of the diffusion depends therefore on the temperature. Diffusion is a microscopic process, which is demonstrated by the Brownian motion or random walk of very small particles. The flux of solutes dn/dt driven by diffusion is described by Fick's law of diffusion (in 1 dimension):

$$\left(\frac{dn}{dt}\right)_{diff} = -A * D * \frac{dC}{dx} \qquad (2.3)$$

with

$(dn/dt)_{diff}$	diffusive flux of solute
A	area of membrane pores, which the flux penetrates
D	diffusion coefficient of solute
dC/dx	concentration gradient

In dialysis the plasma concentration C_p of a solute is separated by the membrane from the dialysate concentration C_d. Their distance dx is defined by the wall thickness s of the membrane. This gives an approximation of the gradient:

 doi:10.20944/preprints202602.0325.v1

$$\left(\frac{dn}{dt}\right)_{diff} = A * D * \frac{C_p - C_d}{s} = \frac{D}{s} * A * \left(C_p - C_d\right)$$

The diffusive flux is counted positive, when the concentration in plasma is higher than in dialysate. This generates a solute transport from plasma to dialysate. With the definition of the permeability k_0

$$k_0 := \frac{D}{s} \tag{2.4}$$

and the definition of the mass transfer coefficient k_0A:

$$k_0 A := k_0 * A \tag{2.5}$$

follows the important result for the diffusive mass transport:

$$\boxed{\left(\frac{dn}{dt}\right)_{diff} = k_0 A * \left(C_p - C_d\right)} \tag{2.6}$$

The mass transfer coefficient k_0A of dialyzer membranes are usually experimentally determined, considering the actual geometry of the pores and that diffusion in porous media is slower than in the bulk of the solvent.

Convection is the solute transfer by the bulk movement of the solvent. The solute molecules are extremely small particles which are dragged on and moved in the same direction as the flow stream. The convective flux is given by:

$$\left(\frac{dn}{dt}\right)_{con} = \frac{dn}{dV} * \frac{dV}{dt} = C * Q$$

or

$$\boxed{\left(\frac{dn}{dt}\right)_{con} = C_p * Q_f} \tag{2.7}$$

with

$(dn/dt)_{con}$	convective flux of solutes
C_P	plasma concentration of solute
Q_f	filtration flow rate

The ratio of the convective and diffusive fluxes gives:

$$\frac{(dn/dt)_{con}}{(dn/dt)_{diff}} = \frac{Q_f * C_p}{k_0 A * \left(C_p - C_d\right)}$$

Neglecting the dialysate concentration C_d results to:

$$\boxed{\frac{(dn/dt)_{con}}{(dn/dt)_{diff}} \approx \frac{Q_f}{k_0 A} = Pe} \tag{2.8}$$

The ratio of the fluxes is identical with the Peclet number Pe. It represents the criterion which flux is more efficient in a clinical setting. When

- Pe < 1 ($Q_f < k_0A$): diffusive flux is predominant,
- Pe > 1 ($Q_f > k_0A$): convective flux is predominant,
- Pe ≈ 1 ($k_0A \approx Q_f$): diffusive and convective flux are equally potent.

Dialyzers of a model series are usually assembled with the same kind of capillaries, which have identical permeabilities k_0. Their mass transfer coefficient k_0A varies with the number of the installed capillaries and is thus proportional to the membrane surface A of the dialyzer. In Figure 2.2 is the impact conspicuously depicted for a small (FX40), a medium (FX60) and a large (FX100) area dialyzer.

The thermodynamic law of equipartition of energy states that, in thermal equilibrium, the energy is shared equally among all molecules. They have the same translational kinetic energy, which means that the motion of the molecules is the slower the higher their molecular masses are. This hampers the diffusive mobility and leads to declining mass transfer coefficients with higher molecular masses. Figure 2.2 shows the steady decline of the k_0A for heavier molecules.

 doi:10.20944/preprints202602.0325.v1

The k_0A fit functions of the 3 dialyzers are extrapolated to the molecular mass of albumin (M = 67kDa).

The traction of the solvent on solute molecules does not depend on their masses. Convective solute transfer is independent of molecular weight and depends solely on solvent drag as filtration rate (Qf) and the sieving coefficient. Therefore, the filtration rate Q_f is depicted in Figure 2.2 as a horizontal line, indicating a constant mass transfer characteristic at a typical filtration rate of Q_f = 100 ml/min.

It is intriguing that diffusion is a much more potent transport vehicle than convection for low molecular weight solutes up to M = 1000 Da. The diffusive clearance for urea (60 Da) or creatinine (131 Da) is a magnitude superior to that of convection. The gain of clearance is nearly negligible in this molecular class when switching from HD to HDF treatment. The dialysate flow rate can be reduced in HDF by substitution flow rate, because for the clearance of these small molecules it doesn't matter whether the dialysis fluid enters the dialyzer as dialysate through the inlet or as filtrate through the membrane. This means when in HDF the total flow rate of dialysate and substitution fluid equals the dialysate flow rate in HD at least the same removal of small molecules is achieved. Usually, the urea clearance in HDF exceeds that in HD by about 5% - 10% under this condition (46). Therefore, in modern HDF treatments there is no difference in the consumption of water, energy and dialysis concentrates compared to HD treatments [47].

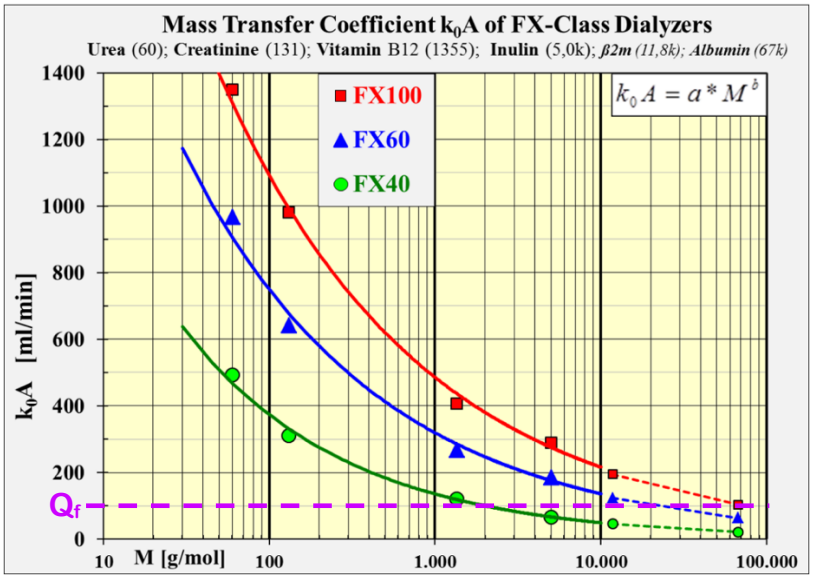

Figure 2.2. Mass transfer coefficients of dialyzers with identical capillaries as a function of the molecular mass M, measured in saline solutions. Membrane areas: FX40: 0.6m²; FX60: 1.4m²; FX100: 2.2m². Dotted lines: extrapolation of fit function in the molecular range from ß2m to albumin. Pink line: filtration rate of Q_f = 100 ml/min.

Diffusion can compete in medium size dialyzers (FX60) with convection up to the middle molecular weight range of about 20kDa. In large size dialyzers (FX100) this range is expanded up to the molecular weight of albumin (67kDa). The performance of free diffusion is amazing. But the solute transfer is hampered in modern dialyzers above a molecular mass of about 10 kDa because the molecules cannot pass the smaller pores of the membrane anymore due to their sizes. It has a detrimental impact on the diffusive as well on the convective transport mechanism, when the molecular size is comparable to the pore diameter. But as diffusion is characterized by a random-walk motion of the molecules it is more restricted than in convection, in which the solutes are dragged and carried along with the solvent flow. With increasing molecular mass, the efficacy advantage tilts to the convective transport.

 doi:10.20944/preprints202602.0325.v1

2.4.2. Solute Transfer Associated to Back Transfer (Diffusion and Filtration) Mechanisms: Benefits and Risks

The solute transfer on the membrane is not a one-way street. If the concentration on the dialysate side is higher than on the blood side, the substance is transferred by diffusion with the identical mass transfer coefficient k_0A from dialysate into blood (back diffusion). The same applies to convective transport, when the filtration flux (back filtration) is reversed by negative pressure differences across the membrane in hollow-fiber dialyzers used with HD machines equipped with fluid-balancing systems [25–27].

Both on the blood and the dialysate side of the dialyzer pressure gradients are present along the capillaries. They are established by the flow resistances R_b on the blood and R_d on the dialysate side of the dialyzer and the corresponding flow rates Q_b and Q_d. The flow resistance R_b is usually the much bigger one because of the higher viscosity of blood and the narrow flow path inside of the lumen of the capillaries.

The course of the local pressures inside the hollow-fiber dialyzer is shown in Figure 2.3 and is typical for high-flux membranes in HD and for low-flux membranes with small ultrafiltration rates, because the transmembrane pressure is very low (TMP≈0). At blood inlet (dialysate outlet) there is higher pressure on the blood side generating a forward ultrafiltration rate. The opposite conditions are present at the blood outlet (dialysate inlet), where lower pressure on the blood side generates a backward ultrafiltration rate. Forward and backward filtration rates are commensurate, as long the TMP is small compared to the pressure drops along the capillaries.

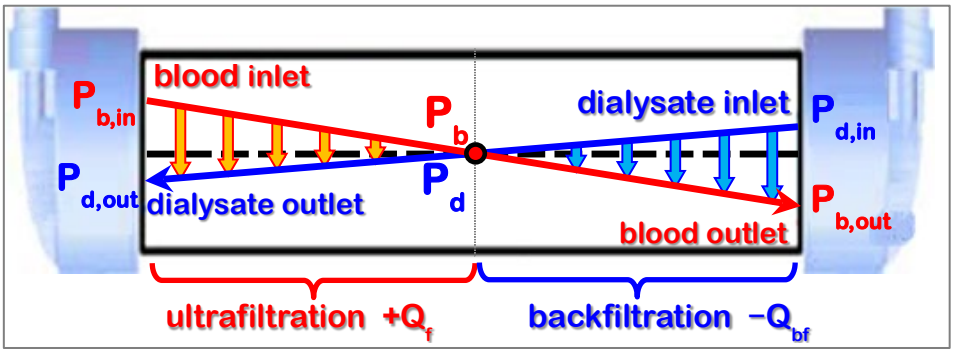

Figure 2.3. Pressure gradients along the capillaries drive the internal ultrafiltration When the external ultrafiltration rate is small $Q_{uf} \approx 0$, forward Q_f and backward Q_{bf} filtration rates are equal (fluid volumes are balanced by the hydraulics).

The backfiltration flow rate increases with higher ultrafiltration coefficient K_{uf} and higher flow resistances on the blood R_b and dialysate R_d side. The backfiltration fraction FF_{bf} can be estimated by Equation (1.7), when dialysate and blood flow rates are similar and the oncotic pressure p_b is negligible.

$$FF_{bf} = \frac{Q_{bf}}{Q_b} \approx \frac{1}{8} * K_{uf} * \left(R_b + R_d\right) \tag{2.9}$$

For high-flux dialyzers with a narrow lumen diameter of 185 mm of the capillaries results a backflow rate of about Q_{bf} = 30 ml/min at a blood flow rate of Q_b = 400 ml/min. FF_{bf} is similar for all dialyzers of a model series with identical fibers, because the K_{uf} is proportional to and the flow resistor R_b is inversely proportional to the number N of the capillaries (R_d is usually negligible).

Standard dialysate, which is not ultrafiltered, is non-sterile and may contain endotoxins. The germs can normally not penetrate the membrane due to their sizes, which exceed the pore sizes by far. But endotoxins can consist of lipopolysaccharides (LBS) (M_{LBS} = 10kDa) and of lipid A (M_{lipidA} = 1.8kDa). The Peclet number determines whether diffusion or convection dominates the transfer of endotoxins in the high-flux dialyzer FX60.

 doi:10.20944/preprints202602.0325.v1

$$Pe_{lipidA} = \frac{Q_{fb}}{(k_0 A)_{FX\,60;1.8kDa}} = \frac{30}{240} = \frac{1}{8} \qquad Pe_{LBS} = \frac{Q_{fb}}{(k_0 A)_{FX\,60;10kDa}} = \frac{30}{120} = \frac{1}{4}$$

Both Peclet numbers indicate that diffusion is the more potent transfer mechanism for endotoxins. High flux membranes were conceived to enable the elimination of uremic solutes in the middle molecular range. As an inherent side effect, the necessity of larger pores led to much higher filtrate rates, which increase with the power of 4 of the pore size according to Hagen-Poiseuille's law. Larger pores increase also the backflow rates, but the solute transfer by backfiltration remains small compared to the prevailing diffusion. Therefore, it is not effective to reduce the backfiltration rate in order to minimize the endotoxin load of the patient. The most efficient method is to apply ultrapure dialysate with accordingly low endotoxin counts (<0.03 EU/mL). As a result, both back-diffusion and backfiltration lose their relevance regarding the microbiological risk for the patient. The use of ultrapure dialysate is mandatory in high-flux dialysis, when caring about the long-term well-being of the patients. This is addressed in the standard ISO 23500 series for water / concentrates for dialysis, dialysis fluid and guidance for the preparation of fluids for hemodialysis and related therapies (51).

2.5. Conditioning of the Synthetic Membrane by a Protein Layer: Mechanisms and Implications

2.5.1. Tightly Fixed Attached Secondary Membrane – Vroman Effect

Blood is a very intricate fluid if it is taken to an extracorporeal system. When any artificial material is in contact with blood, proteins from the blood plasma are adsorbed onto the material surface. According to the Vroman effect these proteins may be displaced by a series of other plasma proteins, all within a time scale of minutes. The sequence of adsorption runs from proteins present at higher concentrations in normal plasma to proteins of lower concentrations, but with high binding affinities:

- albumin
- immunoglobulins (IgG)
- fibrinogen and fibronectin
- factor XII and HMWK

In the end a layer of plasma proteins covers the surface, which profoundly changes the characteristic of the artificial membrane. This protein layer sticks firmly to the basic membrane and cannot be removed even by intense rinsing along the capillaries or transmembrane flushing.

2.5.2. Reduction of Ultrafiltration Coefficient (K_{UF}) and Sieving Coefficient (SC)

Table 2.1 contains the ultrafiltration coefficients (K_{UF}) of low-flux dialyzers, F6 and F8, and of high-flux dialyzers, F60 and F80. They were measured before (aqueous K_{UF} sterile) and after (K_{UF} with protein layer) the membranes were covered with a plasma protein layer. When the ultrafiltration coefficients were determined in forward filtration (saline from blood to dialysate side) a minor reduction was found for the low-flux membranes, but a considerable change for the high-flux membranes. This indicates a strong flow restriction of water by the protein layer. When the ultrafiltration coefficients of the protein-coated membranes were determined in backward filtration (saline from dialysate to blood side) comparable reductions were found for low-flux and high-flux membranes as in forward filtration. This confirmed that the protein layer cannot be removed by rinsing back through the membrane.

 doi:10.20944/preprints202602.0325.v1

Table 2.1. Ultrafiltration coefficients measured in forward and in backward filtration for dialyzers with and without a protein layer [28]. Back flushing the membrane with saline solution didn't restore the sterile K_{UF}!

Type of dialyzer	Forward filtration			Backfiltration		
	K_{UF} sterile (aqueous) ml/h mmHg	K_{UF} with protein layer ml/h mmHg	reduction factor	K_{UF} sterile (aqueous) ml/h mmHg	K_{UF} with protein layer ml/h mmHg	reduction factor
F6	6.0	5.1	1.2	5.7	5.5	1.0
F8	8.0	5.6	1.4	7.3	6.4	1.1
F60	144	57.0	2.5	163	53.5	3.0
F80	163	69.0	2.4	176	48.0	3.7

The temporal built-up of the protein layer in high-flux dialyzers can be monitored by the albumin loss into spent dialysate over time. When the membrane comes initially in contact with blood plasma it has a high permeability even for large proteins like albumin, which implicates a comparably high albumin loss into dialysate (see Figure 2.4). Characteristically, during the first 20 min to 40 min the albumin loss falls sharply and reaches a steady state with nearly constant loss until the treatment ends. The initial albumin peak counts for about 50% of the total albumin loss per treatment [29]. An important feature of HDF machine lies in the way TMP is managed through dedicated algorithms, such as proprietary AutoSub+ function (e.g., Fresenius Medical Care, Bad Homburg, G). This system tightly controls membrane protein layer formation by limiting high ultrafiltration flow during the initial phase of HDF, thereby preventing excessive albumin loss, which otherwise occurs predominantly within the first hour of treatment. This example illustrates the benefits of the interaction membrane properties and HDF machine technology in optimizing HDF performance [58].

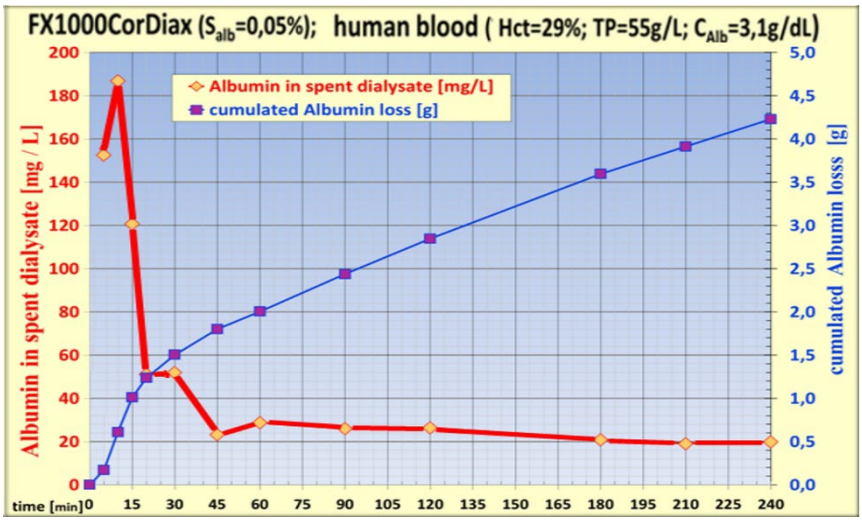

Figure 2.4. Temporal albumin loss into dialysate during a simulated post-dilution HDF treatment.

A plain model is depicted in Figure 2.5 showing the build-up of a protein layer blocking the passway of large molecules. The pristine membrane has a host of large pores whose diameters are still larger than the size of the relevant plasma proteins. This allows an easy protein transfer across the membrane into the spent dialysate, which explains the high initial protein loss. Over time proteins stick to the inner surface of the capillaries and the pores, reducing their free diameter. Plasma proteins are now blocked or hampered to cross the membrane. Once a complete mono layer of proteins is established the process of protein adsorption on the surface is finished. A steady state is reached in which the remaining protein transfer happens through pores being still big enough.

 doi:10.20944/preprints202602.0325.v1

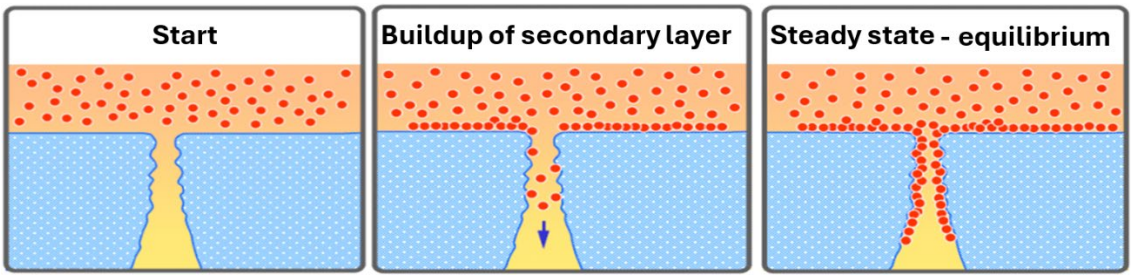

Figure 2.5. Model of secondary membrane build-up and blocking of large molecule.

The build-up of protein layer does not only curtail the albumin transfer, but the exchange of all solutes with molecular sizes in the cut-off region of the membrane. The cut-off region (COR) characterized by the sieving coefficient S is shifted to smaller protein sizes.

Figure 2.7 depicts the sieving coefficient of the high-flux dialyzer FX60 in the cut-off range. It shows the sieving coefficient of the pristine membrane (PSC, blue line) and the modified sieving coefficient after 20 min in contact with blood plasma (SC_{20}, red line). The changes below the onset of the cut-off region (M < 10 kDa) are negligible. Inside the cut-off region the relative change of its sieving coefficient S is more pronounced depending on the molecular weight.

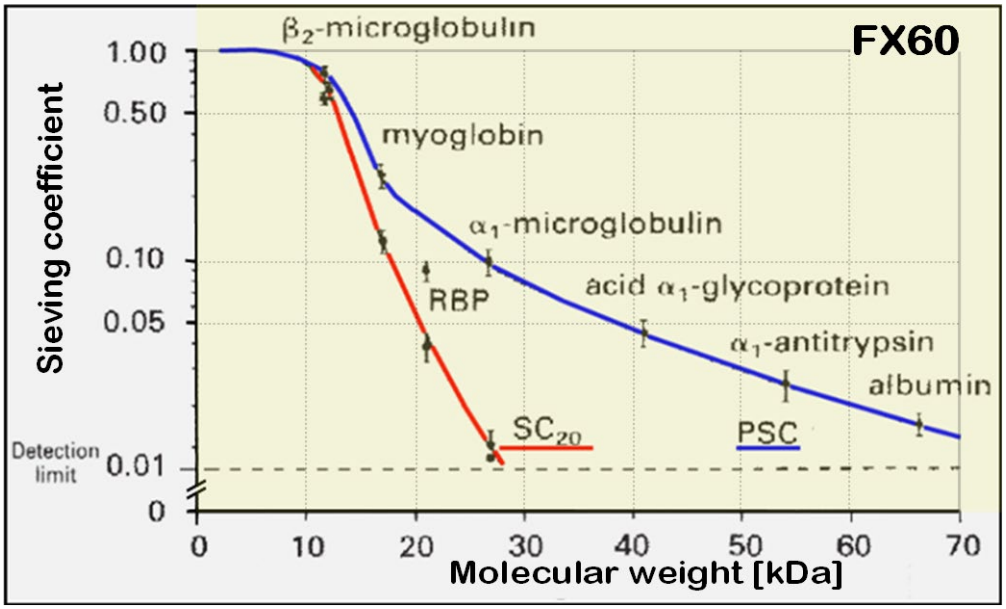

Figure 2.7. Sieving coefficient and protein layer formation on high flux polysulfone dialyzer FX60 (30).

2.5.3. Clinical Consequences of the Protein Layer: Changes in Nominal Permeability

The initial reduction of the ultrafiltration coefficient of high-flux membranes is dramatically high (see Table 2.1), but it has no relevant impact on the treatment. In HD with a rather high ultrafiltration rate of Q_{uf} = 1000 ml/h the TMP rises from 7 mmHg of the pristine membrane with an $K_{UF,1}$ = 150 ml/h/mmHg to 20 mmHg with a resulting $K_{UF,2}$ = 50 ml/h/mmHg due to the established protein layer. The TMP increase is negligible and is comparable to the tolerance of the TMP measurement in dialysis machines.

Even the colloid osmotic pressure (COP) of the blood, which adds to the TMP, is usually bigger than the TMP contribution caused by the dynamic pressure drop across high-flux membranes. This is also valid in post-dilution H(D)F treatments, as will be shown later.

The ultrafiltration coefficient K_{UF} of high-flux membranes has a low significance as performance parameter for the removal of uremic solutes and should not be considered as a relevant criterion for the choice of a dialyzer.

 doi:10.20944/preprints202602.0325.v1

The build-up of a protein layer curtails the exchange of all solutes with molecular sizes in the cut-off region of the filter from ß2m up to albumin. The sieving coefficient S as specified in the dialyzer IFU is valid only after conditioning of the membrane with plasma proteins. The standards EN1283 and ISO8637 require as test fluid anticoagulated bovine or human blood plasma with a total protein concentration of TP = (60 ± 5) g/L and a plasma filtration fraction FF_P of 20%. Surprisingly, the exposure time is not defined despite being a strong confounder.

For the K_{UF} specification the standards require bovine or human blood with a hematocrit of H = (32 ± 2)% and a total protein concentration of TP =(60 ± 5)g/L as test medium.

In contrast to the K_{UF} the steepness of the cut-off curve (see Equation (2.2)) can be utilized as an essential performance parameter for the efficacy of high-flux membranes regarding the removal of middle molecules. A steeper sieving curve is achieved with a tighter pore size distribution allowing better delimitation of solutes, which will be removed and which will be retained in plasma.

A further essential performance parameter is given by the sieving coefficient of albumin $S_{alb.}$ It serves as upper limit for the removal of large middle molecules, so that the loss for proteins like albumin remains in a safe range.

Today, plasma filtration fraction of FF_P = 50% are common in high-volume HDF. As the apparent sieving coefficient usually increases with the filtration rate, the loss of albumin and proteins of comparable size can be quite different between test and treatment conditions.

The specification of the albumin sieving coefficient usually marks not the typical, but the upper limit value, which a dialyzer family may have. A specified value of S_{alb} = 0.1% means that much smaller values like S_{alb} = 0.01% meet the specification as well. The albumin loss in a clinical trial with the same patients can differ by a factor of 10, when dialyzers from the same type, but different manufacturing batches are used.

Dialysis fluid or saline can be used for the clearance determination of small molecules, like urea, creatinine, phosphate, vitamin B12, inulin, or little middle molecules can be used, as their sieving coefficients are not hampered by the protein layer.

2.5.4. Antithrombotic Management of the Dialyzer and Extracorporeal Circuit: Unfractionated Heparin (UFH) Vs. Low Molecular Weight Heparin (LMWH)

Unfractionated heparin (UFH) has been the anticoagulant of choice for many years, but it is replaced more and more by low-molecular-weight heparins (LMWHs). LMWHs are produced by depolymerization of UFH and have a typical molecular weight of about M = 4 - 6 kDa. They show a distribution in terms of chain length, molecular weight and charge.

Whereas UFH are usually administered with an initial bolus followed by a constant infusion rate, LMWHs are administered as a single bolus at the start of the treatment. The anticoagulants are infused into the arterial blood line, up-stream of the dialyzer. During the first dialyzer passage a large part of LMWH is not yet bound to antithrombin due to the excess bolus concentration. This leads to significant LMWH losses (up to 20% – 30%), because in this initial phase the dialyzer membranes are not yet protein coated, which renders them highly permeable for free heparin.

Although most LMWHs are currently recommended for the administration in the arterial line, post-dialyzer administration into the venous line would avoid unnecessary losses of the LMWH dose into the dialysis fluid [55]. The optimal bolus would be administered into the arterial or venous needle before the patient is connected to the extracorporeal circuit.

If not compensated by the bolus dosage, the invisible loss of LMWH is leading to a higher amount of residual blood in the dialyzer, falsely interpreted as a high coagulation activity of the dialyzer.

2.6. Potential Risks Associated with Dialyzer Sterilization Modalities

One crucial step in the production of dialyzers is the sterilization process. To deactivate microorganisms often means to damage materials as well. ETO gas sterilization can be classified as comparatively harmless in this respect; however, degassing requires time and residual amounts of

 doi:10.20944/preprints202602.0325.v1

ETO migrating out of the potting material during dialysis have often led to patient reactions. Radiation with Gamma or X-rays by either a Gamma radiation or e-Beam source are alternative methods which require careful evaluation of potential material damage. Break-down products will remain inside the dialyzer and must be eliminated by the priming / rinsing process. Inline steam sterilized filters show low levels of any type of residues since the sterilization goes along with the active elimination of any production residues or migrating substances.

3. Mechanisms Occurring Within the Dialyzer Membrane During HDF: Understanding Internal Processes

HDF distinguishes itself from HD by the build-up of an additional secondary membrane on top of the protein layer inside the capillary, which is mobile depending on the blood flow rate and is modulated in thickness by the substitution rate. The following chapter tells the story of that secondary membrane.

3.1. Transmembrane Pressure and Protein Polarization at the Membrane

The protein concentration on the membrane can be estimated by a simple model with dead-end filtration, i. e. for the sake of simplicity there is no cross flow on the feed side of the dialyzer (Q_b=0). The focus is on the conflicting effects of the filtrate flow building-up the secondary membrane and the diffusion trying to remove it in order to level out the concentration gradient.

The build-up of secondary membrane is driven by convective flow rate Q_f, which carries the protein flux dn_p/dt to the dialyzer membrane:

$$\left(\frac{dn_p}{dt}\right)_{con} = C_p * Q_f \tag{3.1}$$

with C_p plasma protein concentration
Q_f filtration or substitution flow rate

The large proteins cannot penetrate the membrane (S = 0) but accumulate on the surface establishing a concentration gradient inside the capillaries. This provokes a diffusive flux of proteins back into the plasma bulk, which can be described as follows:

$$\left(\frac{dn_p}{dt}\right)_{diff} = -A * D * \frac{dC_p}{dx} \tag{3.2}$$

The equilibrium is reached when the total flux $(dn_p/dt)_{total}$ of the diffusive and convective transport disappears:

$$\left(\frac{dn_p}{dt}\right)_{total} = \left(\frac{dn_p}{dt}\right)_{con} + \left(\frac{dn_p}{dt}\right)_{diff} = C_p * Q_f - A * D * \frac{dC_p}{dx} = 0$$

The solution of this ordinary differential equation is given by:

$$C_{mem} = C_{bulk} * e^{\frac{Q_f * R}{A * D}} \tag{3.3}$$

with C_{mem} protein concentration on the membrane surface
C_{bulk} protein concentration in the bulk of the plasma
R inner radius of the capillaries
A membrane area
D diffusion coefficient of protein

The following example shows the extent of the protein polarization C_{mem} at the membrane is determined by the balance between convective transport to the surface and diffusion back into the bulk solution.

Example: ultrafiltration rate Q_{uf} = 120ml/min, radius of capillary R = 100 um, membrane area A = 2 m^2, diffusion coefficient of albumin $D_{alb} = 6*10^{-11}$ m^2/s.

Result: C_{mem} / C_{bulk} = 5.3

 doi:10.20944/preprints202602.0325.v1

This example under extreme conditions illustrates that the protein concentration at the membrane surface can be several times higher than the bulk concentration. Under treatment conditions with cross flow on the blood side, the protein polarization is smaller since proteins of that layer are carried out of the capillaries together with the blood flow.

A picture of more realistic flow conditions inside the dialyzer is shown in Figure 3.1. The plasma proteins are flowing inside of the blood flow stream Q_b tangential to the membrane surface. The high ultrafiltration flow rate Q_f perpendicular to the membrane surface conveys the proteins to the surface of the membrane. Depending on their size they are retained and concentrated, still moving along the capillary as indicated by the red arrows. The protein polarization layer represents a moving secondary membrane of proteins whose concentration increases with distance from the blood inlet due to the increasing extracted UF volume.

The blood flow rate Q_b is driven by a pressure gradient generated by the blood pump along extracorporeal circuit. The higher shear stress produced by this flow entrains concentrated large molecules and keeps them moving to the blood outlet. If the ultrafiltration flow rate Q_f stops, the whole polarization layer will be washed out with a rinsing volume comparable to the dialyzer blood volume.

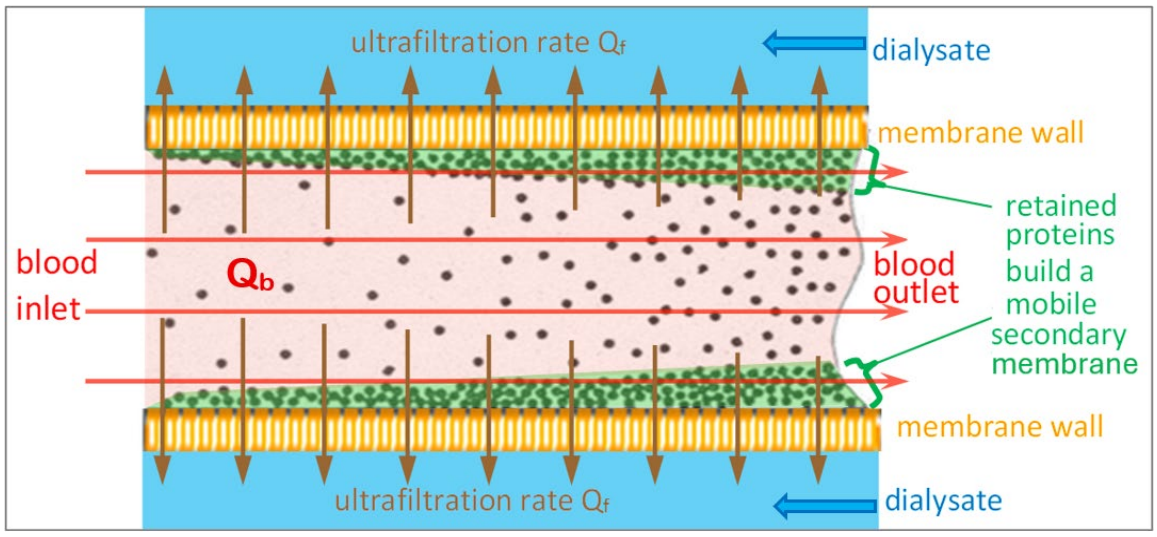

Figure 3.1. Flow and transport conditions inside of the dialyzer capillary. Generation of the mobile secondary layer on the membrane by retained proteins.

To gain a deeper insight into the characteristics of the secondary layer, a 3-dimensional model of the dialyzer has been developed. The intriguing conclusion shows the true nature of the transmembrane pressure.

The model comprises 3 different flow domains – blood, inner volume of the membrane, dialysate – based on the Navier–Stokes law:

$$\frac{\partial \vec{v}}{\partial t} + (\vec{v} \circ \nabla)\vec{v} = \frac{\eta}{\rho} * \Delta \vec{v} - \frac{1}{\rho} * \nabla P + \vec{g} \qquad (3.4)$$

It is derived from the equilibrium of forces between inertial mass, internal friction, pressure gradients and gravity on a finite volume element. The solution gives the local velocities $\vec{v}$ and the local pressures P inside the 3 domains of the dialyzer.

The motion and concentration build-up of the proteins (C_P) and blood cells (hct) were simulated by the general transport equation:

$$\frac{\partial C}{\partial t} + \vec{v} \circ \nabla C = D * \Delta C \qquad (3.5)$$

 doi:10.20944/preprints202602.0325.v1

It considers the convective and diffusive transport characteristics. The velocity $\vec{v}$ of the convection is obtained from the Navier-Stokes equation Equation (3.4). However, the changed local concentrations, varying local viscosities ⊚ and densities ⊚,⊚have a direct influence on both velocity and pressure profiles. Therefore Equation (3.4) and Equation (3.5) must be solved iteratively (numerical CFD solver of ANSYS-CFX).

The main result was the ultrafiltration characteristic of a dialyzer in HDF treatment. It described the TMP necessary to push the ultrafiltration flow rate Q_f across the membrane and could be very well described by the Starling Equation (32):

$$Q_{uf} = K_{uf} * (TMP - \pi_b) \quad (3.6)$$

with K_{uf} ultrafiltration coefficient of the dialyzer with protein layer [ml/min / mmHg]

TMP transmembrane pressure [mmHg]

p_b colloid osmotic pressure (COP) of the blood plasma proteins [mmHg]

The COP was calculated by the Landis-Pappenheimer equation (33, 34):

$$\pi_b = 2.1 * C_p + 0.16 * C_p^2 + 0.009 * C_p^3 \quad (3.7)$$

with: ⊚b colloid osmotic pressure (COP) of plasma proteins [mmHg]

C_p total protein concentration in plasma [g/dl]

The amazing finding was that the colloid osmotic pressure ⊚b of the plasma proteins in Equation (3.6), calculated by the Landis-Pappenheimer equation was sufficient to yield an excellent agreement between model and observation, even in the very high concentrations of the polarization layer.

The COP is a phenomenon at a semi-permeable membrane, which can be passed by the solvent (water) but not by all solutes. At physiologic protein plasma concentrations of about C_P = 7 g/dL the COP has the standard value of ⊚b = 25 mmHg.

Figure 3.2 (bottom) shows the calculated course of the albumin concentration along the capillary in High-Volume-HDF post-dilution. The albumin concentration at the membrane rises steeply directly after blood inlet and reaches 3- to 4-fold bulk level after a short distance. The protein polarization causes colloid osmotic pressure values p_b between 200 mmHg and 380 mmHg (see Figure 3.2 (top)), which are typical TMP readings under HDF conditions. For the COP calculation, local concentrations of the accumulated proteins at the membrane C_{mem} were applied instead of bulk protein concentrations C_{bulk}.

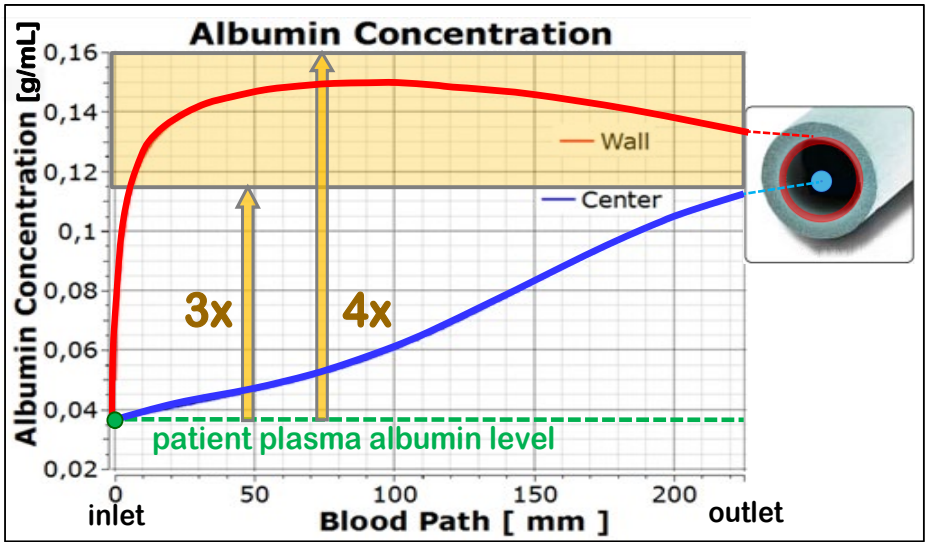

 doi:10.20944/preprints202602.0325.v1

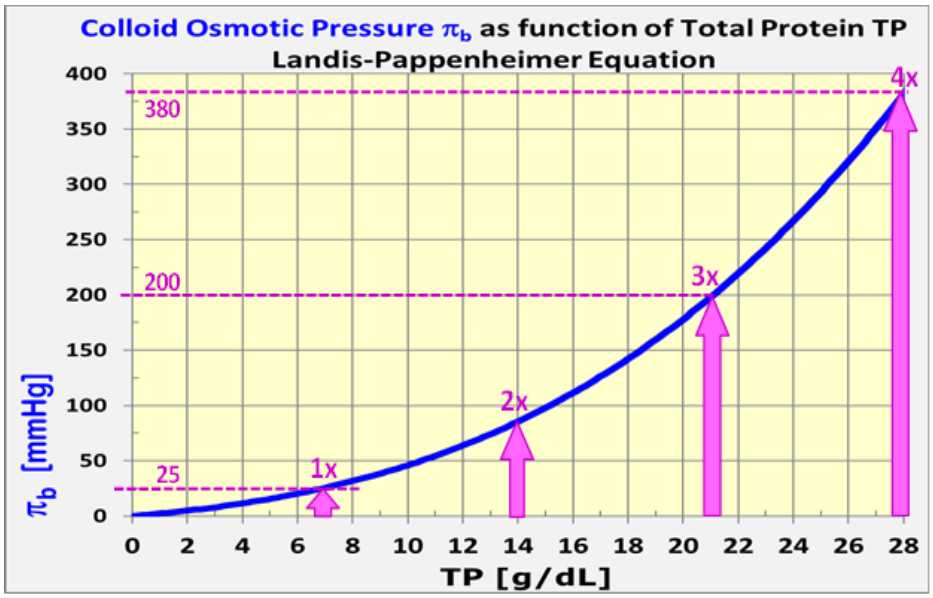

Figure 3.2. Colloid osmotic pressure and plasma protein concentrations inside of the capillary. **top:** Plasma albumin concentrations along the capillary at the membrane (red) and on the axis of the capillary (blue). Simulation Parameters: Q_b = *300ml/min;* $Q_{uf} = Q_{sub}$= *135 ml/min; FF = 45%;* dialyzer*:* FX1000. **bottom:** Colloid osmotic pressure π_b as a function of total plasma protein concentration C_p according to Landis-Pappenheimer up to concentrations reached in protein polarization layer in post-HDF. Arrows indicate oncotic pressures at physiological plasma protein concentration 7g/dl and at twice, thrice and forth-fold levels.

In addition to the colloid osmotic pressure, the dynamic pressure drop across the dialyzer membrane DP_{mem} contributes to the TMP (35).

$$TMP = \Delta P_{mem} + \pi_b \tag{3.8}$$

The dynamic pressure drop ΔP_{mem} pushes the ultrafiltration fluid Q_f through the pores of the membrane and is given by:

$$\Delta P_{mem} = Q_f / K_{uf} \tag{3.9}$$

The reciprocal value of the ultrafiltration coefficient $1/K_{uf}$ corresponds to the flow resistance of the membrane R_{uf}. Since the flow inside of the membrane wall is laminar due to the very small dimensions of the pores, the pressure drop ΔP_{mem} increases proportionally with the ultrafiltration flow rate Q_f (see: Figure 3.3, yellow line). Forward filtration starts as soon as the TMP has overcome the COP π_0 of the blood. With increasing filtration rates Q_f the protein polarization at the membrane surface and the associated COP increase $D\pi_b$ raises progressively leading to a total COP π_b of

$$\pi_b = \pi_0 + \Delta\pi_b \tag{3.10}$$

The corresponding ultrafiltration characteristic Q_f vs. TMP of a FX 800 dialyzer is shown in Figure 3.3. Zero net ultrafiltration rate $Q_f = 0$ is achieved at a transmembrane pressure of TMP = π_0 to counteract the oncotic pressure of blood plasma. The non-linear ultrafiltration characteristic of high-flux membranes is a consequence of the protein polarization and the resulting high oncotic pressure π_b at the membrane (by Landis-Pappenheimer), which is always several times higher than the pressure drop ΔP_{mem} across the membrane and prevails the total transmembrane pressure TMP.

 doi:10.20944/preprints202602.0325.v1

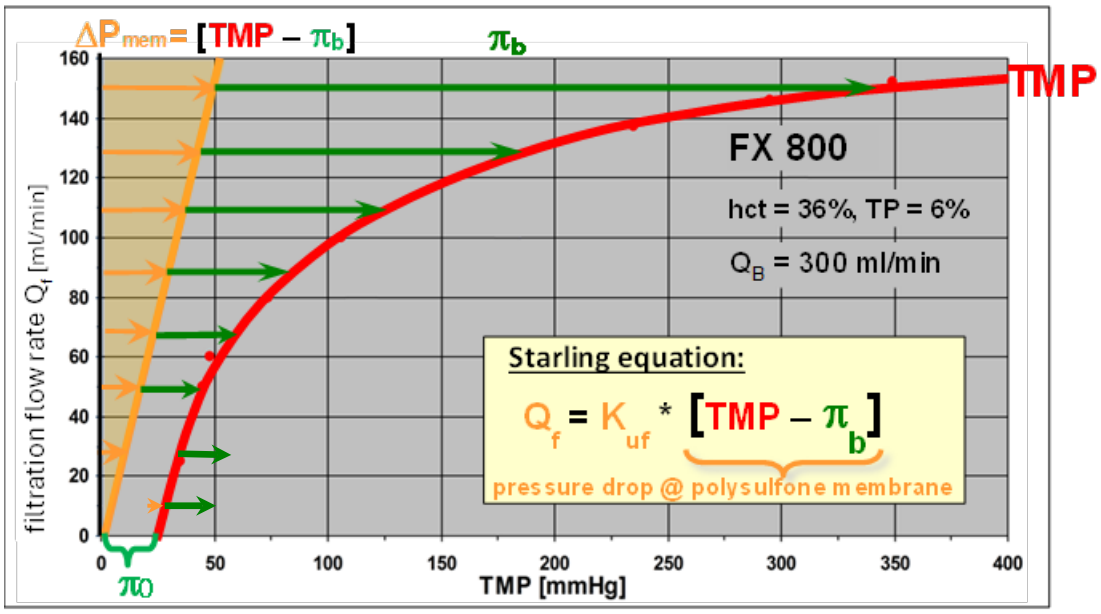

Figure 3.3. Ultrafiltration characteristic of high-flux membranes. The oncotic pressure $\varpi_b = \varpi_0 + \Delta\varpi_b$ of the plasma proteins at the membrane determines the behavior. ΔP_{mem} is the pressure drop across the membrane.

The viscosity inside of secondary membrane is elevated due to the protein polarization and it generates an additional flow resistance for the plasma conveyed to the membrane by the filtrate rate. But surprisingly, the resulting pressure drop on top of the TMP is completely negligible, because the secondary membrane spreads across the entire membrane area [typical 2 m²] and has a very thin layer thickness [a few micro-meter]. Additionally, the velocity of filtration fluid v_f is extremely slow (e. g. Q_f = 120 ml/min, A = 2 m² => $v_f = Q_f / A$ = 1 um/s).

3.2. Changes in Ultrafiltration Characteristics (KUF) During HDF Treatment

The ultrafiltration coefficient (K_{UF}), which reflects changes in the hydraulic permeability of the membrane, is influenced by blood composition and by changes in blood volume (hemoconcentration) during treatment resulting from net ultrafiltration, vascular refilling rate and the patient's weight loss to correct fluid overload. The prescribed weight loss causes blood thickening, and the increasing protein concentration leads to a higher colloid oncotic pressure (COP), resulting in a higher transmembrane pressure (TMP) at the same filtration rate.

The concomitant change of the K_{UF} is shown in Figure 3.4 in a concrete example. The treatment starts at a Hct = 36% and TP = 6 g/dL (K_{UF}: red line). After the 4 h treatment, the blood composition changes to Hct = 41% and TP = 7.5 g/dL (K_{UF}: blue line). In HDF treatment with a constant exchange rate Q_f (yellow arrows) of e. g. 120 ml/min the TMP reading is about 160 mmHg at the beginning and about 300 mmHg at the end of the treatment. This is a shift of 140 mmHg in 4h or 35 mmHg in 1h.

Whereas in HD the TMP drift is negligible due to the small ultrafiltration rate Q_{uf}, it is clearly visible in HDF. Higher exchange rates Q_f are intrinsically linked with a marked increase of the TMP drift, but at the same time the convective clearance of middle molecules is far more efficient – the central purpose of HDF treatments. Unfortunately, very high initial exchange rates Q_f can lead to excessive TMP drifts during the treatment, which will trigger machine alarms. Therefore, the optimal convective clearance is reached with exchange rates, which ensure that the TMP stays just within the alarm limits.

 doi:10.20944/preprints202602.0325.v1

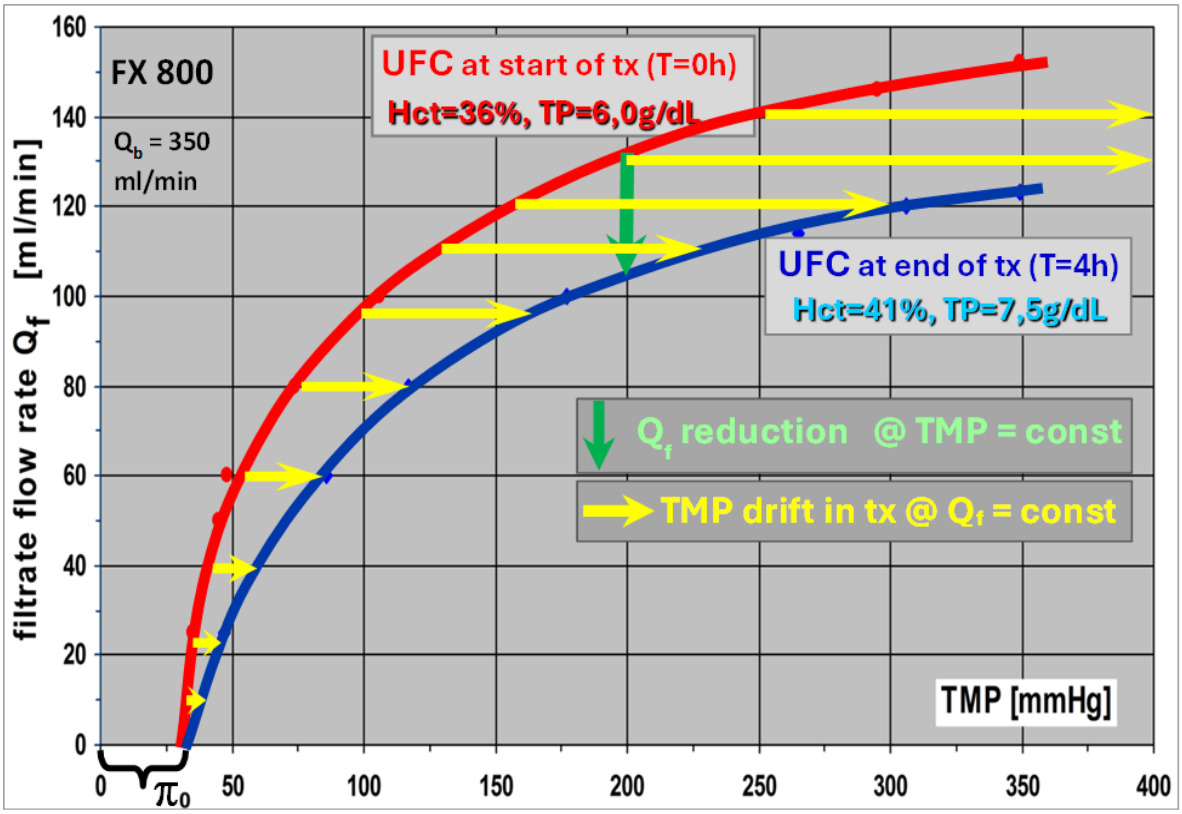

Figure 3.4. Ultrafiltration characteristic (UFC) of high-flux membranes for different blood compositions. red line: UFC at *hct = 36%* and *TP = 6.0 g/dL* (start of treatment) blue line: UFC at *hct = 41%* and *TP = 7.5 g/dL* (with weight loss at end of treatment) yellow arrows: TMP drifts at constant filtrate flow rates Q_f green arrow: reduction of filtrate flow rate Q_f at a constant TMP of 200mmHg.

HDF treatments with TMP control would be an alternative modality. The substitution rate Q_f is controlled by the machine to keep a preset TMP value constant. For a chosen TMP of 200 mmHg in this example (see Figure 3.4, green arrow), the substitution rate Q_f is reduced from initially 130 ml/min to 105 ml/min during the treatment. This more conservative mode prevents excessively high TMPs at the end of the treatment in all cases.

For the clinician, the challenge remains in selecting the optimal prescription in manual mode, either a constant exchange rate (Q_{sub}) or constant TMP, to achieve the best treatment efficiency.

3.3. Hemoconcentration Due to Excessive Transmembrane Pressure (TMP) and Ultrafiltration Rates

As described above, high ultrafiltration rates may cause high protein polarization on the membrane. Acute hemoconcentration may occur if the protein flux arriving at the membrane via convection cannot be removed by diffusion and blood flow. This situation causes a sudden, steep increase in the protein polarization (see Figure 3.5) which is marked by an abrupt and dramatic TMP surge, with characteristic rises of up to 100 mmHg/min (see Figure 3.5).

An additional factor contributing to excessive hemoconcentration is high net ultrafiltration with a low vascular refilling rate, reflecting substantial weight loss. This leads to a relative blood volume contraction of more than 10%, resulting in a marked increase in blood viscosity [36].

The recommended approach to managing this issue is to reduce or, preferably, temporarily stop the substitution rate Q_{sub} for a few minutes. This action halts further protein polarization, allowing the concentrated blood within the dialyzer to be cleared with the ongoing blood flow Q_b. As a result, the dialyzer's flow and pressure flow characteristics are restored.

In all cases, it is essential to maintain a high blood flow rate to exert strong shear stress on the membrane. This shear stress effectively "scrubs" the membrane, reducing the thickness of the protein layer and preventing excessive protein polarization.

 doi:10.20944/preprints202602.0325.v1

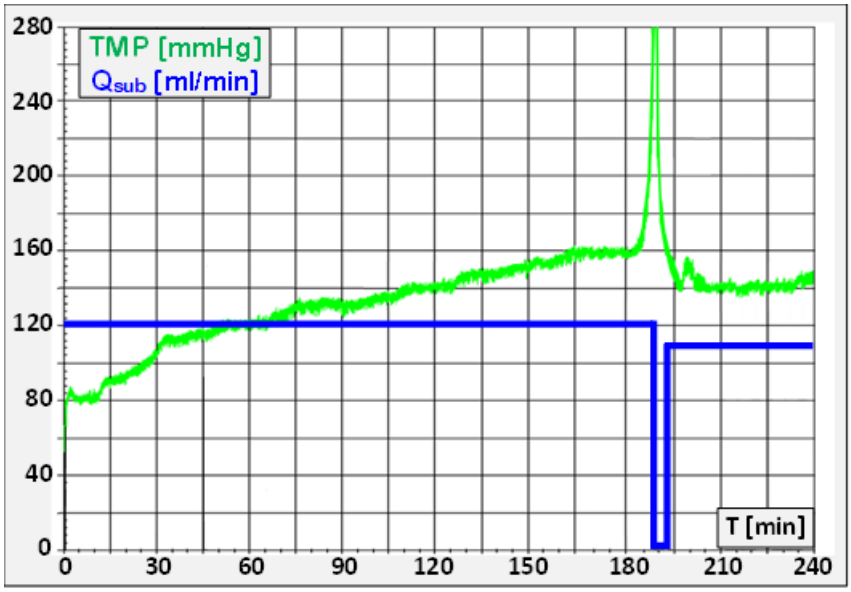

Figure 3.5. TMP drift in HDF post-dilution with constant substitution rate Q_{sub}. Occurrence of an acute hemoconcentration after about 190 min.

Acute hemoconcentration and clogging should not be confused with blood clotting in the extracorporeal circuit, although both conditions typically trigger TMP alarms as well as venous or arterial pressure alarms. The usual response to clotting involves increasing the heparin dose or, in some cases, discarding blood-filled lines and/or dialyzers. However, these actions do not resolve the underlying issue in cases of hemoconcentration and could result in significant blood loss, worsening the patient's condition. Therefore, it is essential to accurately identify the cause of the alarms, as acute hemoconcentration generally occurs far more frequently than blood clotting.

The pursuit of the optimal High-Volume-HDF treatment conditions leads to an unavoidable predicament: convective volumes of >23L are required for highly efficient treatments but leading to an increased risk of sudden hemoconcentration events. It is even worse, since the hemoconcentration cannot be anticipated and the rapid pressure changes leave no time for the nurse to interfere adequately.

Consequently,

- the prescribed convective volume is not reached,
- the dialysis efficiency for middle molecules is reduced,
- the workload for the nurses is higher due to more interventions,
- the albumin loss is increased due to high TMPs.

This implicates that automatic control algorithms in the dialysis machines are needed, which determine continuously the stress inside the dialyzers and adjust the substitution rate accordingly. It must include a sensitive scouting monitor for the onset of hemoconcentration in combination with a rapid intervention procedure. In that way, the maximum exchange rates can be achieved under stable treatment conditions avoiding intra-dialytic trouble.

3.4. HDF Increases the Removal of Middle and Large Middle Molecules in a Convective Dose-Dependent Manner

Several recent clinical trials [6,37–40] and meta-analyses [7,8,41] have shown, that HDF treatments generate an improved patient outcome only when convective volumes larger 23 L have been achieved. This observation raises the question, what makes High-Volume-HDF superior to normal HDF or HD. Which kind of molecules are removed more efficiently by this technique compared to the others? The answer to this question may give also a hint where unidentified uremic toxins might be hidden.

 doi:10.20944/preprints202602.0325.v1

It is well known that HDF does not notably improve the removal of small uremic solutes. In modern dialyzers with a sieving coefficient for ß2m of $S_{ß2m} > 0.8$ this comprises small middle molecules up to 12kDa. The ß2m mass removal increases by only 11% changing from HD to HDF and another small 10% changing from HDF to High-Volume-HDF as shown in Figure 3.6.

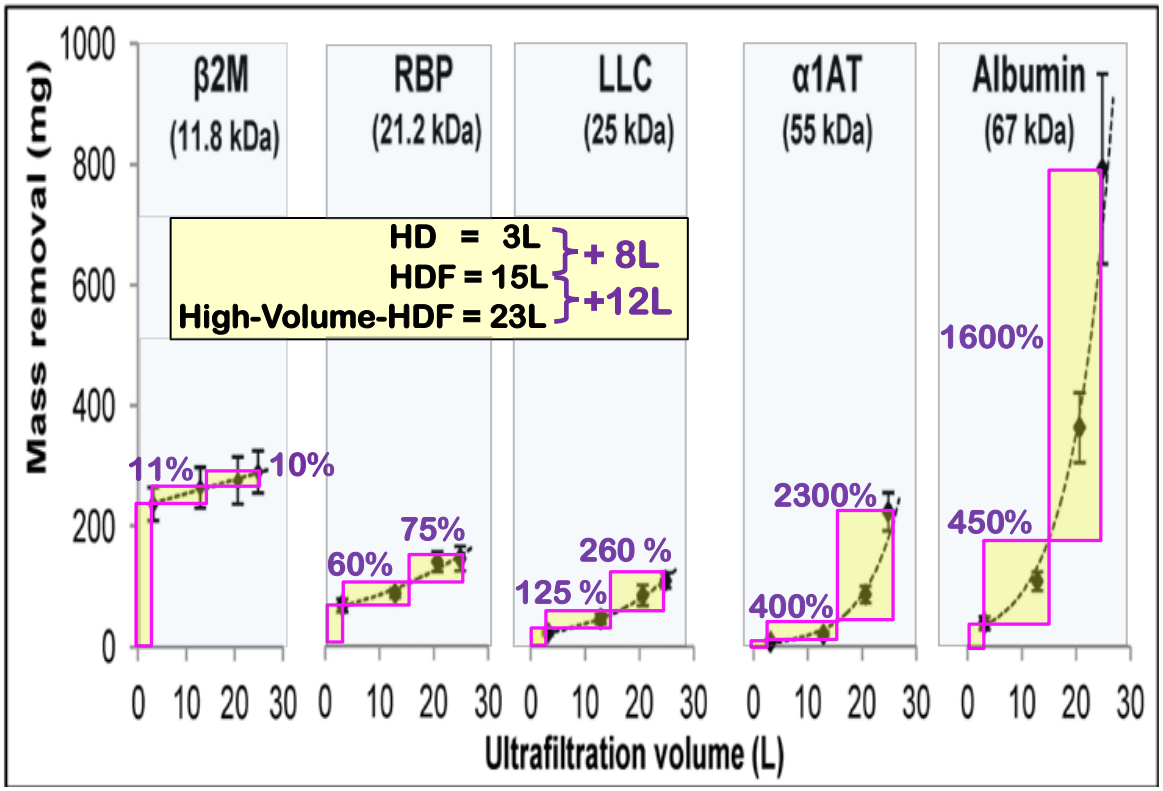

Figure 3.6. Increased mass removal with higher molecular weight and higher exchange volumes. HD with weight loss of V_{UF}=3L, *HDF* with *15L* convective volume (12L exchange volume + *3L* V_{UF}); High-Volume-HDF with 23L convective volume (20L exchange volume + 3L V_{UF}) [42].

Beyond 12kDa the removal efficiency improves dramatically with increasing molecular weight. The observation can be explained by effects:

(a) Convection gets more efficient than diffusion as transport mechanism. One reason lies in the molecular mass of the proteins which are in size comparable to the membrane pores. Another reason is given by the advantage of directed convective solute transport in narrow pores compared to an undirected diffusive motion.

(b) Solutes with smaller sieving coefficients are retained largely by the membrane and form a dense protein layer. Their concentrations in the polarization layer increase exponentially with the filtration rate and cause the non-linear characteristic of the solute removal gain.

With this removal behavior in mind, it is very important that the upper limit of the albumin sieving coefficient of high-flux membranes is very small, typically around 0.1%. Thus, the removal is very limited in this molecular range, despite the huge relative concentration increase at higher exchange volumes. Finally, the effect on the albumin levels of the patients is negligible.

That leads to the conclusion, that in the molecular range between ß2m (11.8kDa) and albumin (67kDa) High-Volume-HDF is the superior treatment modality. As High-Volume-HDF generates a survival benefit for the patients, it can be hypothesized that the responsible uremic toxin(s) can be found in that molecular range, consisting of proteins like cytokines, hormones and adipokines. They are involved in chronic inflammation, atherosclerosis and heart diseases, which are the main causes of high mortality rates in dialysis patients.

 doi:10.20944/preprints202602.0325.v1

3.5. Risk of Albumin Loss in High Volume HDF

Albumin is not classified as a uremic solute and the plasma levels in dialysis patients are often below physiological range. While albumin losses cannot be totally avoided in dialysis treatments the removal shall not reach unsustainable amounts. The scientific community has not yet established an agreement about the tolerable albumin loss per treatment. The discussed limits are very diverse and range from 3g (in Europe and Western World) up to 12g (in Asia and Japan Region) per session.

The main stimulus of the albumin loss is the substitution rate in company with the inherently built-up of the secondary membrane and the sieving coefficient of the membrane. It must be considered, that the sieving coefficients specified in the IFUs of dialyzers are measured at a plasma filtration fraction of FF_P = 20% according to the standards (ISO 1283, ISO 8637), but that in High-Volume-HDF much higher plasma filtration fractions like FF_P = 50% are common and that the apparent sieving coefficient under such clinical conditions can be several times higher, as shown in Figure 3.7 at higher exchange rates. That amplifies the albumin loss (see Figure 3.6).

When the filtration fraction FF_P is controlled by the dialysis machine to maximize the exchange volumes the potential albumin loss must be kept in mind. The optimum middle molecule removal in combination with a safe albumin loss is accomplished by matching the cut-off characteristic of the filter and the algorithms of the dialysis machine to create an optimal holistic approach.

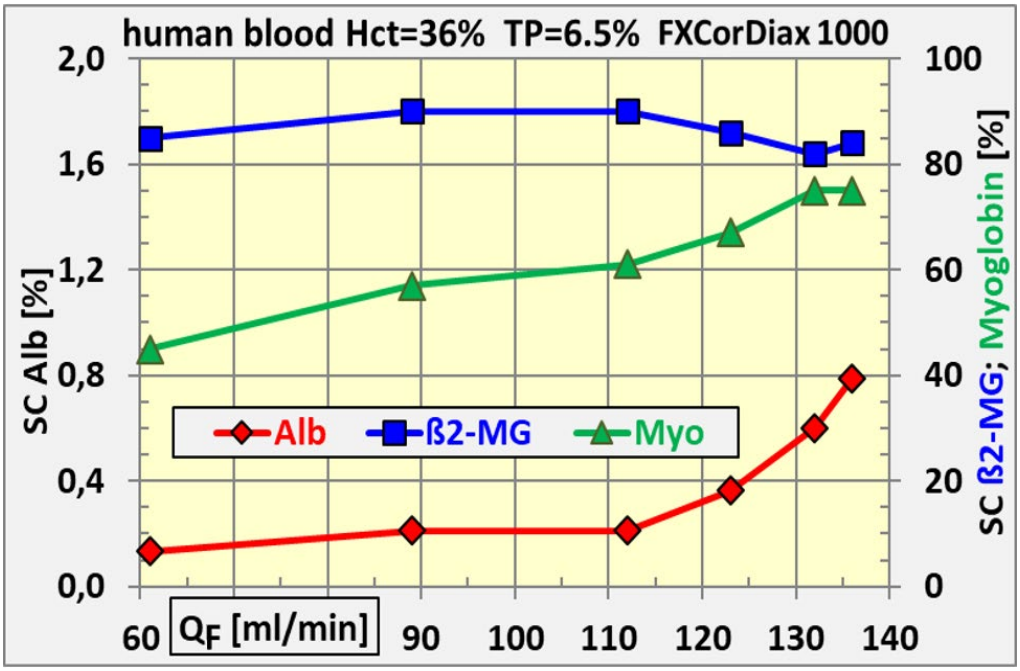

Figure 3.7. Sieving coefficient of different proteins as a function of filtration rate Q_f. Note the high relative increase of S_{alb} at high filtration rates.

The ultrafiltration coefficient K_{UF} is often taken as a criterion for choosing a high-flux dialyzer. Comparing the dialyzers ELISIO-H™ and SOLACEA-H™ (Table 3.1) shows that a higher ultrafiltration coefficient does not necessarily imply higher sieving coefficients. The disparity of sieving coefficients of both series is considerable especially for large middle molecules. A rough estimation of the albumin losses m_{alb} in High-Volume-HDF post-dilution for both filters yield:

SOLACEA-H™: $m_{alb} = S_{alb} * C_{alb} * Q_f * T = 0.013 * 40g/L * 120ml/min * 4h = 15.0g$

ELISIO-H™: $m_{alb} = S_{alb} * C_{alb} * Q_f * T = 0.002 * 40g/L * 120ml/min * 4h = 2.3g$

The significant difference between potentially critical and tolerable albumin losses could not be derived from the ultrafiltration coefficients.

 doi:10.20944/preprints202602.0325.v1

Table 3.1. Comparison of UFC and sieving coefficients of 2 dialyzer series.

Type (area)	**Ultrafiltration coefficient** [ml/h / mmHg]	
	ELISIO-H	**SOLACEA-H**
15H (1.5m²)	67	61
17H (1.7 m²)	74	69
19H (1.9 m²)	76	72
21H (2.1m²)	82	76
25H (2.5m²)	93	87

Molecule (MW [kDa])	**Sieving coefficient** [1]	
	ELISIO-H	**SOLACEA-H**
Vitamin B12 (1.4)	0.989	1.00 .
Inulin (5.2)	0.926	1.00 .
ß2m (11.8)	0.803	0.85 .
Myoglobin (17.0)	0.223	0.80 .
Albumin (67.0)	0.002	0.013

3.6. Substitution Modalities (Pre-, Post- and Mixed-Dilution HDF) and Their Implications

Various substitution modalities have been developed to overcome clinical limitations of post-dilution HDF. The substitution pump infuses ultrafiltered, sterile and non-pyrogenic fresh dialysate from the volume-balancing system into patient's blood. If the infusion site is upstream of the dialyzer, the blood is pre-diluted and if it is downstream of the dialyzer, it is post-diluted. In both cases, the balancing system retrieves the extracted volume across the dialyzer membrane as an additional filtration rate. The TMP is increased by lowering the hydraulic pressure until the filtration flow rate compensates for the extracted infusion rate.

In post-dilution plasma water together with all permeable ingredients is removed. Thus, the filtration rate $Q_{f,post}$ is equivalent to the convective clearance for large molecules. Typically, 50% of the plasma water flow rate Q_{pw} can be exchanged. The blood cells and the residual proteins are concentrated accordingly inside the capillaries.

To achieve the same convective clearance in predilution, the infusion rate $Q_{f,pre}$ must equal the plasma water flow Q_{pw}, i. e. twice the value of post-dilution: $Q_{f,pre} = 2 * Q_{f,post}$. The uremic plasma solutes are distributed in the doubled plasma water volume of which 50% is extracted in the dialyzer. In predilution treatments with high blood and high plasma water flow rates respectively, the high fluid volumes exceed the filtration capacity of the membrane. In this case post-dilution would be superior, due to the smaller filtration rates of undiluted plasma water. Additionally, the concentration gradients of small molecules are not diluted, preserving a high diffusive clearance of small uremic solutes.

In treatments with low plasma water flow rates and large dialyzers, there is more filtration capacity than needed for the equivalent filtration rate in predilution. Under these conditions, pre-dilution would be superior, because more than 50% of the plasma solute can now be extracted by convection. Additionally, the frequency of hemoconcentration and the risk of unsustainable albumin losses is much less pronounced.

Patients with high hematocrit can be preferably treated with online-HDF pre-dilution as well, because of the lower plasma water flow fraction. In summary, the break-even between pre- and post-dilution depends on blood flow rate, hematocrit and dialyzer surface.

In Mixed-HDF the total substitution flow rate is administered in a pre- (≈1/3 Q_{sub}) and in a post-dilution (≈2/3 Q_{sub}) fraction. Depending on the rheological constraints inside of the dialyzer the dialysis machine delivers the convective volumes more in pre- or in post-dilution mode. The procedure generates always optimal treatment conditions adapted for each patient's individual physiology.

3.7. Comparison of High-Volume External HDF and Internal HDF in MCO Membranes

The combination of medium cut-off (MCO) membranes with internal filtration (i.e. Expanded HD, HDx) as well as high-volume hemodiafiltration (High-Volume-HDF) focuses specifically on enhancing the removal of large middle molecules. In this range of molecular masses, both free diffusion and free convection contribute equally to solute transport. However, closer to the cut-off region of the membranes convective transport is more efficient than diffusion since the mobility of

 doi:10.20944/preprints202602.0325.v1

large molecules in narrow pores is restricted. To avoid the reduced removal efficacy, the share of larger pores must be increased, which makes high demands on the control of the fiber spinning process. Rather small shifts in the cut-off curve lead to significant changes in elimination efficiency. If the cut-off curve is not firmly reproducible in serial production, dialyzers from different lots will show a wide spread variability in reduction rates [15]. In addition, internal filtration depends strongly on blood flow, hemorheologic conditions, and blood flow resistance, making it highly dependent on operational conditions. Furthermore, the MCO dialyzer functions as a 'black box', with no meaningful or sample method to verify that the prescribed convective dose has actually been delivered, in contrast with online HDF.

This could be an explanation for the observation of different reduction rates of large middle molecules of 2 MCO dialyzers of the same family (Table 3.2) with different surface areas. The MCO dialyzer with the smaller area showed a higher reduction rate in the whole middle molecular range. Especially at the upper end were the differences more pronounced including the higher albumin loss.

Table 3.2. Reduction of middle molecules and albumin loss in Expanded HD. [43,44].

Reduction rate of middle molecules and albumin loss	MW [kDa]	**Theranova 400™** 1.8 m²	**Theranova 500™** 2.0 m²
ß2-microglobulin	12	78%	74.7%
Myoglobin	17	68%	62.5%
k–free light chains / Prolactin	23	**70%**	**60.0%**
YKL-40 / a1-glycoprotein	40	**63%**	**2.8%**
loss of albumin	67	**3.0 ± 0.2 g/Tx**	**0.03 ± 0.01 g/Tx**

High-Volume-HDF can also be affected by variation of the average pore size, but the changes might be less profound, because convective transport and the built-up of an enhanced secondary protein layer can partially compensate for these differences. Furthermore, membranes with intended use of HDF have generally a more conservative molecular cut-off.

Solute removal by convective transport is also present when MCO membranes are utilized, driven by internal filtration. The internal filtration fraction FF_{bf} can be estimated by Equation (2.9), because internal filtration and back-filtration are identical. As the MCO and high-flux dialyzers have comparable UFCs and lumen diameters of 185 mm, there is no difference in their respective FF_{bf}. Typical backflow rates are 30 ml/min at a blood flow rate of 400 ml/min. In HD mode the gain in large middle molecular clearance of MCO membranes is higher as direct result of their larger sieving coefficients.

The mechanism of internal filtration depends strongly on the blood composition and viscosity of the individual patient. At the same time, the blood viscosity determines the flow characteristics through the hollow fiber as described by the fundamental law of Hagen–Poiseuille:

$$R_b = \frac{\Delta P_b}{Q_b} = \frac{128}{\pi} * \frac{\mu * L}{D^4} \qquad (3.11)$$

where Q_b blood flow rate,
ΔP_b axial pressure drop,
μ blood viscosity,
L fiber length, and
D diameter of the lumen.

An increase in flow resistance R_b leads to a proportional increase in the axial pressure drop that is required to convey the blood flow through the capillaries. The hematocrit increases the viscosity μ of the blood [45], which is proportional to the flow resistance.

Blood with a low hematocrit contains a large plasma water fraction, which could be utilized to enhance the convective removal. But the internal filtration fraction is low in MCO membranes due to

 doi:10.20944/preprints202602.0325.v1

the low blood viscosity and the concomitant little flow resistance R_b. The passive control of the filtration rate leads to patient individual convective treatments, but not to optimized removal rates.

When patients with high hematocrits are treated, the resulting large flow resistance forces stronger internal filtration. Due to the limited amount of plasma water, the ensuing concentration of blood leads to even further filtration and may even cause a final blocking of the fibers.

In contrast, automatic algorithms in actively controlled High-Volume-HDF treatments sense the stress in the dialyzer and modulate the filtrate flow rate according to the present pressure and flow conditions. This yields a patient individual filtration rate with an optimal convective clearance, independent of the blood rheology of the patient.

4. Key Characteristics of the Optimal HDF Membrane

4.1. Optimal Membrane Characteristic

Although the detailed aspects an optimal membrane for HDF application have been discussed in preceding chapters, they are described here again in a comprehensive summary.

(1) The steepness of sieving coefficient curve.

High flux dialysis membranes are characterized by the pore size distribution and the resulting function of the sieving coefficient curve with increasing molecular weight. The optimal characteristics would correspond to the natural example of the kidneys (biomimicry), because the elimination ratio of medium sized proteins would match the physiological needs of a healthy subject. Like the steepness of the sieving curve of natural kidneys, the steepness represents an essential performance parameter for HDF dialyzers as well. Despite all improvements, the pore size distributions of modern membranes have achieved this ideal goal of the kidney function only partially.

(2) Restricting the albumin elimination.

The choice of the sieving coefficient of albumin by the upper end of the pore size distribution defines the second essential performance parameter. Additionally, the albumin elimination is modulated by the treatment conditions, i. e. the sieving coefficient must be specified according to the intended use. For High-Volume-HDF in post-dilution, membranes must have a more conservative limit than for HD or HDF in pre-dilution.

(3) Lumen diameter and fiber length.

Since the convective filtrate volume is actively controlled by the dialysis machine, the internal filtration depending on the dimensions of the fiber is not required to achieve effective convective clearance. Therefore, there is no need to narrow the lumen diameter or increase the length of the fiber for HDF membranes. On the contrary, a larger lumen diameter can be selected in HDF, which reduces blood shear stress inside the dialyzer and mitigates internal filtration phenomena that may hinder ultrafiltration flow and solute clearance.

(4) Ultrafiltration coefficient K_{UF} and plasma water permeability.

The primary development goal of high-flux membranes was to increase the pore sizes to allow an adequate middle molecular clearance. As a mere side effect, the larger pores caused a disproportional increase of the water permeability according to the law of Hagen-Poiseuille.

The comparably low filtration rates in post dilution cause only a small dynamic pressure drop, correlated to the ultrafiltration coefficient K_{UF}, which leads to a rather small TMP contribution. Due to the high protein polarization, the TMP is dominated by colloid osmotic pressure. Therefore, water permeability or K_{UF} plays a minor role.

In pre-dilution high filtration rates cause far higher dynamic pressure drops across the membrane, which predominates the TMP. Lower protein polarizations in pre-dilution lead to reduced colloid osmotic pressures. Hence, the water filtration capacity determined by the membrane area of a high-flux dialyzer is important.

 doi:10.20944/preprints202602.0325.v1

4.2. Currently Available HDF Dialysis Membranes

The key characteristic of high-flux membranes used for Online-HDF consist of a steep cut-off characteristic and an albumin sieving coefficient restricting the albumin loss to an acceptable level (see Section 2.5.3). The most suitable membrane materials meeting these requirements are synthetic copolymers, where polysulfone (PS) and polyethersulfone (PES), mixed with hydrophilic polyvinylpyrrolidone, play a predominant role (>90%). The remaining HDF membranes are made from other synthetic polymers, like polymethylmethacrylate (PMMA) or polyacrylonitrile (PAN) [20].

5. The Gibbs-Donnan Effect and Its Implications for Electrolyte Balance in Post-Dilution Hemodiafiltration

5.1. Concerns of Unforeseeable Na Shifts in HDF Treatments

There are eligible concerns, that in HDF treatments two additional electrolyte transfer mechanisms are induced, which could significantly alter the electrolyte balance. Sodium is of special interest due to its dominant plasma concentration.

5.1.1. Concentration Gradient Between Plasma Water and Substitution Fluid

Due to the Donnan effect, the sodium plasma water concentration is higher than in dialysate, when both sides are in equilibrium. Nevertheless, there is no diffusive sodium transfer through the membrane in this case. In HDF high convective volumes are drawn across the membrane with the higher plasma sodium concentration. The filtrate is replaced by a substitution fluid with the lower dialysate sodium concentration. This concentration gradient in combination with exchange volumes >23 L could induce a significant, non-indented sodium removal in contrast to HD.

5.1.2. Excessively High Donnan Factors by the Protein Polarization Layer

As the strength of Donnan effect is determined by the negative charge of the protein concentration present on the surface of the membrane, the emerging concern has been that the sodium difference in equilibrium could also be increased with the protein layer concentration (see Figure 3.2), totaling up to 28 g/dL. This could cause a Donnan factor of $F_{D,HDF} = 0.80$ and would require a dialysate sodium of $C_{Na.d} = 117$ mmol/l to prevent diffusive Na flux into the blood. The standard dialysate sodium setting of $C_{Na.d} = 138$ mmol/L would 21 mmol/l higher than the equilibrium concentration leading to a high diffusive sodium flux into the patient.

In both cases the dialysate sodium ought to be adjusted in order generate sodium flux over the membrane, which compensates for the convective loss and diffusive gain. The clinicians would have no means to deduce the appropriate dialysate sodium level, which would fit to the momentary treatment conditions. In the end, this would be a huge obstacle for HDF in clinical routine and would require an additional proceeding for an adequate electrolyte balancing.

However, the practice of routine High-Volume-HDF therapy, experimental results and theoretical models confirm that these fears and concerns can be refuted. The theoretical background of the Donnan effect and its impact on HDF will be explained in the following chapters. (56)

5.2. Gibbs-Donnan Effect

The Donnan effect is a surface phenomenon on the interface between blood plasma and dialyzer membrane. The small cationic electrolytes (like Na) of blood plasma can easily enter the dialyzer membrane. Larger proteins, which are mostly negatively charged, cannot follow due to the size exclusion by the small pores. This generates a charge separation. While the membrane surface is positively charged, the plasma layer carries a negative charge. This space-charge region creates an electrical field, which retains cations (Na^+, K^+) and repels anions (Cl^-, HCO_3^-) from the blood plasma (see Figure 5.1). The potential difference U generated by the electrical field establishes a concentration difference between both sides, which can be described by the Nernst equation:

 doi:10.20944/preprints202602.0325.v1

$$-z_i * F * U = R * T * \ln \frac{C_{i,d}}{C_{i,p}} \quad (5.1)$$

with U potential difference on the space-charge region [V],

z_i charge number of ion i [1]

$C_{i.d}$, $C_{i.p}$ concentration of ion i in dialysate (d) and in blood plasma water (p) in Donnan equilibrium, i. e. no diffusive transfer happens [mol/l].

F Faraday constant [96485 As/mol]

R ideal gas constant [8.314 J/mol/K]

T temperature [K]

Separating Equation (5.1) into an ion-specific term (left) and a constant term (right) gives the definition of the Donnan factor F_D:

$$F_D := \left(\frac{C_{i,d}}{C_{i,p}} \right)^{\frac{1}{z_i}} = e^{-\frac{F*U}{R*T}} \quad (5.2)$$

The same Donnan factor F_D applies for all electrolytes i, but each ion has an individual concentration ratio $C_{i.d}/C_{i.p}$ depending on its charge number z_i. The potential difference U is positive for the negatively charged plasma proteins, which gives Donnan factors of $F_D < 1$.

On the semi-permeable dialyzer membrane, the concentrations $C_{i.p}$ of cations ($z_i > 0$), like sodium, are always higher in the blood plasma water than their equilibrium concentrations $C_{i.d}$ on the dialysate side. With a typical Donnan factor in hemodialysis of $F_D = C_{Na.d} / C_{Na.p} = 0.95$ and a plasma sodium concentration of 145 mmol/L the equilibrium sodium concentration in dialysate corresponds to 138 mmol/L, i. e. a sodium difference of 7 mmol/L prevents diffusive sodium transfer. The concentrations $C_{i.p}$ of anions ($z_i < 0$) are always lower in the blood plasma water than their equilibrium concentrations $C_{i.d}$ on the dialysate side (e.g. $C_{Cl.p} = 100$ mmol/L => $C_{Cl.d} = 105$ mmol/L and $C_{bic.p} = 24.0$ mmol/L => $C_{bic.d} = 25.3$ mmol/L).

In complex mixtures like blood and dialysate, the Donnan factor F_D is calculated using the neutrality condition in both domains. Considering the cations sodium (Na), potassium (K), calcium (Ca), magnesium (Mg) and proteins (P) with the charge number z_p. in the plasma water (p), it ensues:

$$F_D = \sqrt{1 - \frac{|z_P| * C_P}{C_{Na,p} + C_{K,p} + 2 * (C_{Ca,p} + C_{Mg,p})}} \approx \sqrt{1 - \frac{|z_P| * C_P}{C_{Na,p}}} \quad (5.3)$$

The Donnan factor F_D depends only on the electrolyte concentrations in the plasma. Dialysate electrolytes have no impact.

5.2.1. The Gibbs-Donnan Effect and High Convective Fluxes in HDF

The distinctive characteristic of this space-charge region is its extremely narrow thickness of about the Debye length l_D, which is less than 1 nm at the ionic strength in plasma or in dialysate. The Debye length l_D is determined by the interaction of thermal and electrostatic energies with the ions. Nevertheless, the charged double layer is responsible for the difference of the sodium concentration between plasma (p) and dialysate (d) of typical $\Delta C_{Na} = C_{Na.p} - C_{Na.d} = 7$ mmol/L. In detail, the Donnan effect can be described also for HDF treatment as follows:

1. Because of the extraordinary narrow thickness of electrical double layer an extremely high sodium concentration gradient of $\Delta C_{Na}/\Delta x = 7$ mmol/L / 1nm = 7000 mol/L / mm exists in the layer. That gradient causes a very high diffusive sodium flux of ($D_{Na} = 1.9 \cdot E\text{-}9 m^2/s$; $A = 1.6 m^2$):

$\Delta N_{Na}/\Delta t = D_{Na} * A * \Delta C_{Na}/\Delta x$

$= 1.9 \cdot E\text{-}9 m^2/s * 1.6 m^2 * 7000$ mol/L / mm

= 76600 mol/h.

The typical solute fluxes are exceptionally high.

 doi:10.20944/preprints202602.0325.v1

2. The negatively charged plasma proteins cannot follow due to their size. A space-charge region is generated in which an electrical field E is established directing from the membrane to the blood compartment. The electrical field $E = U/\Delta x$ generates an electrophoretic flux inside of the double layer, which drives the cations back to the blood compartment and counterbalances so their diffusive flux. The steady state, respective the Donnan equilibrium, is reached, when both fluxes cancel each other out and the net flux is zero.

When the electrolyte concentration in the dialysate is equal to the equilibrium concentration, no diffusive exchange occurs (see Figure 5.1).

3. An additional flux of electrolytes is conveyed in HDF by the convective ultrafiltration flow rate through the membrane. But even at the high filtration rates Q_f achieved in High-Volume-HDF, this convective flux is very small compared to the diffusive flux in the space-charge region.

Example: At a very high exchange rate of Q_f = 120 ml/min the convective sodium flux reaches only:

$\Delta N_{Na}/\Delta t = C_{Na,p} * Q_f = 145$ mmol/L * 120 ml/min = 1 mol/h.

This convective sodium flux is about 5 orders of magnitude smaller than the diffusive sodium flux (and the equal electrophoretic counter-flux). It contributes only to a very weak perturbation of the fluxes created by the Donnan effect and is negligible, therefore. The concentration ratio $C_{i.d}/C_{i.p}$ across the space-charge region, defined by the Donnan equilibrium, is not altered even with the additional convective flux achievable in HDF treatments.

4. When electrolytes are dragged along by a convective filtration rate Q_f inside of the capillary lumen, the fluid has the plasma water bulk concentration, e. g. sodium: $C_{Na.p}$ = 145 mmol/L, until at the onset of the double layer. Since the cations are partially repelled by the electrical field, their concentrations steadily fall along the flow path through the space-charge region. The concentrations in the filtrate flow, leaving the electrical double layer ($l_D \approx 1$ nm), are stripped down to the concentrations of the Donnan equilibrium (48), e. g. sodium: $C_{Na.Donnan}$ = 138 mmol/L.

5. In the case of anions, e.g. chloride: $C_{Cl.p}$ = 100 mmol/L, the electrical field E attracts the negatively charged ions in the plasma and accelerates them in the space-charge region, which steadily increases their concentrations during the passage of the double layer up to the concentrations of the Donnan equilibrium, e.g. chloride: $C_{Cl.Donnan}$ = 105 mmol/L.

6. When the electrolytes leave the double layer, their concentrations are equal to the equilibrium concentrations determined by the Donnan effect, even at very high convective streams of plasma water penetrating the space-charge region in High-Volume-HDF.

7. The Donnan effect ensures that the total flux of all electrolytes reaching the dialysate side of the membrane is electrically neutral.

The concentration profile in the membrane induced by the Donnan effect is illustrated in *Figure* 5.1 for a plasma containing only charged proteins (P^{-p}), sodium (Na^+) and chloride (Cl^-) ions for simplicity. The concentrations of the electrolytes differ between blood and dialysate side, though both sides are in thermodynamic equilibrium. The dynamic equilibrium is established by the diffusive (Diff) and electrophoretic (E) ion fluxes, which are equally strong but moving in opposite directions. The concentration gradient in the double layer does not drive a net flux out of it.

When the dialysate concentration $C_{i.d}$ of an electrolyte is set to the equal concentration as that of the Donnan-equilibrium $C_{i.Donnan}$ no net diffusive flux occurs. Otherwise, e. g. $C_{i.d}$ is set equal to the plasma concentration, the concentration difference drives a diffusive flux (w: wall thickness of membrane, i: ion i) through the membrane:

$$\Delta N_i/\Delta t = D_i * A * (C_{i.Donnan} - C_{i.d})/w \qquad (5.4)$$

The electrolytes in the ultrafiltration fluid have the concentrations set by the Donnan-equilibrium after passage of the double layer. This means that convective volumes do not remove plasma water with electrolytes of plasma concentrations, but with Donnan-equilibrium concentrations. This leads to an accumulation of cations and a deprivation of anions in plasma. The plasma remains electrically neutral because the diffusive and convective fluxes carry no net charges through the membrane.

 doi:10.20944/preprints202602.0325.v1

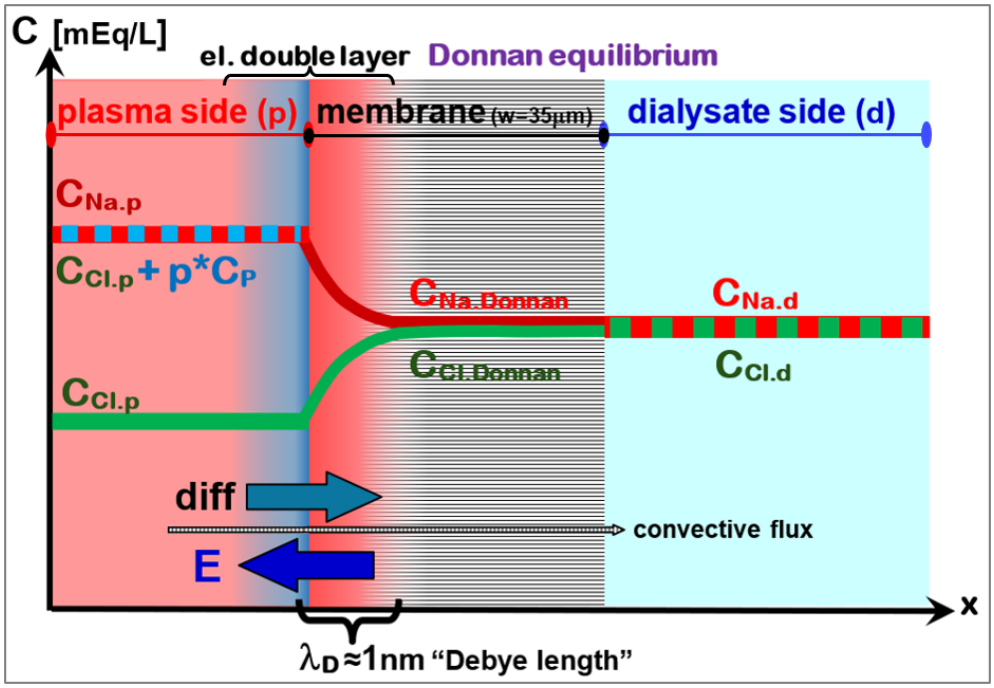

Figure 5.1. Concentration profiles and electrolyte fluxes in the space-charged region under Donnan equilibrium. Arrows indicate diffusive (diff), electrophoretic (E) and convective fluxes of cations. Electro-neutrality condition in plasma (p): $C_{Na,p} = C_{Cl,p} + p * C_P$ Index: Na: sodium $(z_{Na} = +1)$, Cl: chloride $(z_{Cl} = -1)$, P: multiple charged proteins $(z_P = -p)$.

In summary, the convective flow conveys the electrolytes with its plasma concentrations to the electrical-double-layer. The effluent concentrations are changed by the Donnan effect and reach the equilibrium concentrations on the other side of that layer, independent of the filtration rate. If the extracted plasma volume is substituted by dialysate fluid with the equilibrium concentrations the electrolyte balance is not disturbed. This is the answer to the concern formulated in Section 5.1.1.

5.2.2. The Gibbs-Donnan Effect and Protein-Concentration in post-HDF

In treatments with High-Volume-HDF in post-dilution a large part of the plasma water is extracted while the blood is running through the capillaries. As the electrolyte concentrations in the effluent filtration flow has been brought to that of the Donnan equilibrium, which differs by the Donnan factor F_D from the plasma concentrations, the concentrations of the plasma electrolytes change steadily with increasing plasma filtration fraction FF_P. Cations are partially retained, so their plasma concentrations rise. The non-permeable proteins are retained in the residual plasma water, so their plasma concentrations rise, too. Anions are partially expelled from the plasma by the electrical forces, so their plasma concentrations diminish. These independent concentration changes alter the Donnan factor of the plasma (see Equation (5.3) along the capillaries as the filtration fraction increases.

This was the reason for the concern that the electrolyte concentration of the Donnan equilibrium $C_{i.Donnan}$ could change accordingly. If the equilibrium concentration equals the dialysate concentration at the inlet of the dialyzer, both would differ downstream, when the equilibrium concentration changed. This would require an intricate adaptation of the prescription of the dialysate electrolyte composition in order to achieve a therapeutic goal, e. g. to have a zero diffusive electrolyte exchange.

The problem was analyzed in a theoretical model. The target filtration fraction FF_P was sliced into small, finite fractions ΔFF_P to investigate whether under the changing conditions along the capillaries the equilibrium concentrations $C_{i.Donnan}$ of the electrolytes are affected. In every filtration fraction slice ΔFF_P, starting from the blood inlet to the outlet of the dialyzer, the following steps were performed:

 doi:10.20944/preprints202602.0325.v1

(1) The filtration fraction $FF_P(x)$ of the plasma is incremented by a finite amount ΔFF_P.

(2) Calculation of the progressive thickening of bulk plasma proteins C_P in the slice.

(3) Calculation of the changed plasma water concentration of the electrolytes $C_{i,p}$: anions are depleted, and cations are concentrated by filtration due to the concentration gaps between plasma water and filtrate with equilibrium concentrations.

(4) Calculation of the new, decreased Donnan factor F_D.

(5) Calculation of the Donnan-equilibrium concentrations of the electrolytes $C_{i.Donnan}$ on the dialysate site.

(6) Go to step 1 until the target filtration fraction FF_p is reached.

The intriguing result was that the equilibrium concentrations $C_{i.Donnan}$ are not noteworthily changed by the filtration rate Q_f and the consequently altered electrolyte composition of the plasma. The impact remains vanishingly low even at extremely high plasma filtration fractions FF_P up to 0.7, which are not reached even in High-Volume-HDF. As an important result in the clinical routine of HDF treatments follows, there is no need for adjusting the dialysate composition depending on the exchange volume. Thus, the electrolyte balance is not influenced by HDF treatment conditions. This is the answer to the concern formulated in Section 5.1.2.

For further illustration the following example is considered with a simple plasma water and dialysate composition containing only the electrolytes Na^+ and Cl^- . The concentrations at the dialysate inlet equal the Donnan equilibrium concentration referred to the blood inlet composition. The selected input and calculated output concentrations of the electrolytes are shown in Table 5.1 and Figure 5.2 depicts concentrations along the dialyzer capillaries.

Table 5.1. Composition of plasma and dialysate electrolytes used for simulation and results at a filtration fraction of FF_p*=0,50*. (p=plasma, d=dialysate).

Ion i	Na,p	Cl,p	Protein	Na,d	Cl,d	F_D
z_i	+1	-1	-15	+1	-1	- -
$C_{i.input}$ [mmol/L]	146	131	1.0	138	138	0.945
$C_{i.output}$ [mmol/L] @ FF_p= 0.50	154	124	2.0	138	138	0.896

In High-Volume-HDF the plasma fraction removal is typically FF_P = 0.5 as selected in this example. The sodium concentration of plasma water increases from 146 mmol/L to 154 mmol/L while the protein concentration doubles. On the other hand, the plasma water chloride concentration decreases from 131 mmol/L to 124 mmol/L (see Figure 5.2).

At the blood inlet of the dialyzer the electrolytes are in a Donnan equilibrium with a factor of F_D = 0.945. Despite the big concentration changes on the blood side the equilibrium concentrations of 138 mmol/l remain constant for both electrolytes up to the dialyzer blood outlet, where the Donnan factor reaches its lowest value of F_D = 0.896. This is shown by the following calculations: $C_{i.Donnan} = C_{i.p} * F_D^{zi}$

Table 5.2. Calculation of equilibrium concentrations of the Donnan effect at plasma compositions at the inlet and the outlet *(FF_p = 0.50)* of the dialyzer.

electrolyte	blood inlet (FF_P=0,50)	blood outlet	equilibrium concentration
Sodium (Na^+)	146 mmol/L * 0.945 =	154 mmol/L * 0.896 =	138 mmol/L
Chloride (Cl-)	131 mmol/L / 0.945 =	124 mmol/L / 0.896 =	138 mmol/L

The sodium and chloride concentrations in the dialysate are not changed from the selected inlet value of 138 mmol/L along the dialyzer, because they match the Donnan equilibrium concentrations. There is no diffusive electrolyte transfer across the membrane.

 doi:10.20944/preprints202602.0325.v1

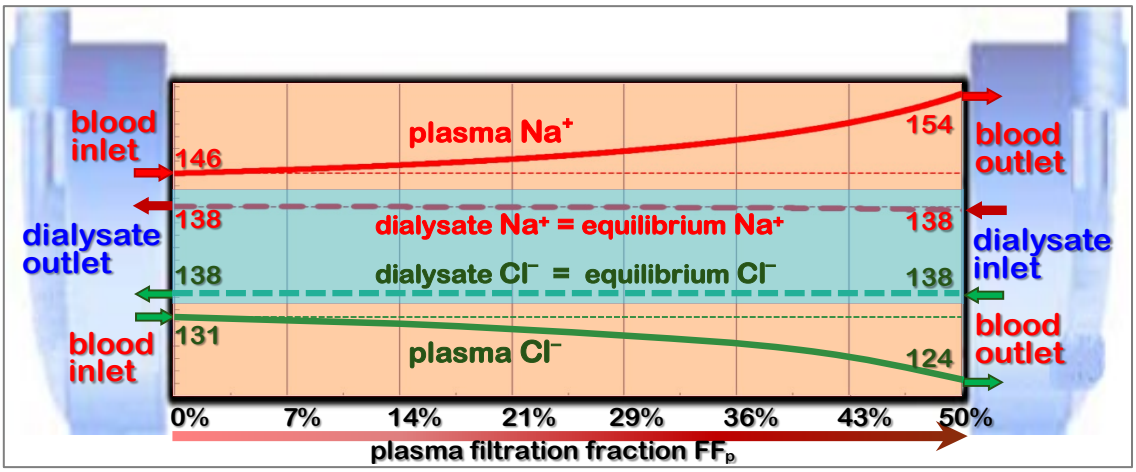

Figure 5.2. Concentration change of plasma water electrolytes along the capillaries caused by the Donnan effect and by filtration (range of plasma filtration fraction FF_P: 0% … 50%) red: changes of plasma and equilibrium concentrations of sodium (cation, $z = +1$) green: changes of plasma and equilibrium concentrations of chloride (anion, $z = -1$)) Donnan factor decreases from blood inlet ($FF_P = 0\%$) to outlet ($FF_P = 50\%$) from 0.945 to 0.896 and the protein concentration doubles as 50% of plasma volume is extracted.

The protein and electrolyte concentration of the blood plasma water at the outlet of the dialyzer differs much from the original plasma composition of the patient, as shown in the data of Table 5.1. However, the concentrated plasma is diluted by infusing substitution fluid downstream of the dialyzer restoring the electrolyte plasma water concentrations to the patient's levels before it is returned.

With a plasma filtration fraction of $FF_P = 50\%$ as in the example above, the volumes of plasma and substitute are mixed in a 1:1 ratio. Dialysate and online-prepared substitute have identical electrolyte compositions. Therefore, the electrolyte concentrations in the plasma after mixing yield the mean concentrations:

$$C_{i,p,mix} = \left(C_{i,p,out} + C_{i,d}\right) / 2 \qquad (5.5)$$

with

$C_{i.p.mix}$ electrolyte plasma water concentrations after mixing,

$C_{i.p.out}$ electrolyte plasma water concentrations at the blood outlet,

$C_{i.d}$ electrolyte concentrations in dialysate.

The concentrations in plasma after mixing (dilution) with substituate can be calculated as follows:

sodium: $C_{Na.p.mix} = (154 + 138)/2 = 146$ mmol/L $= C_{Na,p.0}$

chloride: $C_{Cl.p.mix} = (124 + 138)/2 = 131$ mmol/L $= C_{Cl,p.0}$

protein: $|z_P| * C_{P.mix} = (30 + 0)/2 = 15$ mmol/L $= C_{p,p.0}$

In summary, the plasma water electrolyte concentrations returned to the patient in the venous line are identical to those in the arterial blood. The substitution fluid not only dilutes the concentrated proteins to the patient's levels but resets the plasma electrolyte concentrations back as well.

6. Advancing Membrane Innovation: Future Directions and Emerging Trends

Even under optimistic assumptions, membranes that fully mimic the native kidney's exchange capabilities are unlikely to emerge in the foreseeable future. The active transport of proteins or other solutes in artificial membrane remains unfeasible. However, an innovative approach has been developed in the bioartificial kidney (BAK), where sufficient numbers of active immortalized tubular cell are incorporated into the dialysate compartment, restoring endocrine and metabolic functions. BAK has shown promising results in acute kidney injury patients requiring kidney support, with

 doi:10.20944/preprints202602.0325.v1

notable improvements in outcomes. Yet, its complexity and cost make it impractical for chronic kidney replacement due to scalability challenges.

A more realistic improvement lies in biomimicry, aiming to match the sieving characteristics of artificial membranes to those of native kidneys. To achieve this, retention must be shifted to higher molecular weights, without altering the albumin sieving coefficient, which already mimics that of the native kidneys. This requires the sieving coefficient curve, as shown in Figure 6.1, to be steeper and not just shifted. Another appealing approach to further enhance efficiency of extracorporeal kidney replacement therapy developing multilayer membranes with adsorption capacity focusing on protein bound uremic toxins. Further progress in the field requires continuous efforts to improve the controlled quality of raw materials, such as artificial polymers and solvents, and refine manufacturing processes, including membrane and filter production and sterilization techniques, within economic constraints. While significant strides have been made, only incremental improvements are likely in the near future.

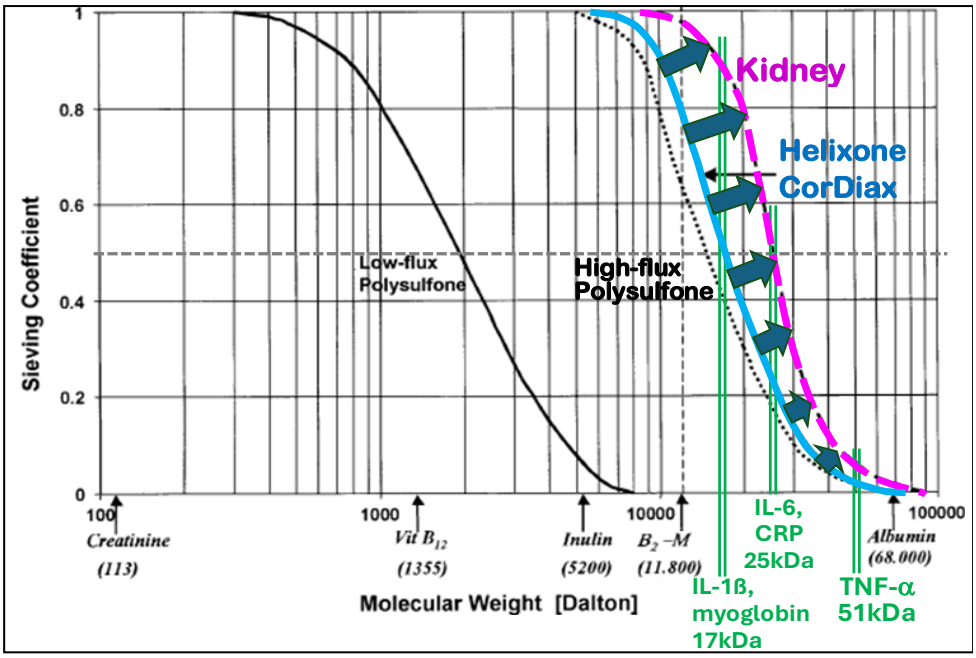

Figure 6.1. Enhancing the removal of large middle molecule by biomimicry of the kidneys.

7. Conclusions

Advanced dialysis membranes, incorporating novel polymers and nanotechnology-based fiber spinning techniques, combined with advanced HDF monitoring technologies, significantly enhance the efficacy of hemodiafiltration by enabling more efficient and selective removal of uremic toxins. Additionally, the hemocompatibility of membranes may be enhanced by modifying the surface-blood interface. Surface modification technologies can create a top layer that reduces the activation of the complement and coagulation systems, potentially eliminating or significantly lowering the need for heparin dosing.

Looking ahead, current technologies are sufficiently mature to enable the production of multilayer hollow fibers, with each layer designed to serve distinct functions. The innermost layer is critical for hemocompatibility, while its pore size distribution determines the molecular cut-off region for middle molecules and the albumin sieving coefficient. Subsequent layers can incorporate adsorptive materials designed to capture a broad range of organic uremic solutes, particularly protein bound uremic toxins. As solutes diffuse through the inner layer, they can be captured within these outer adsorptive layers, offering high clearance efficiency even at relatively low dialysate flow rates. This approach combines diffusive transport with adsorption, from example through the use of activated carbon to bind uremic solutes, including protein-bound compounds. Such adsorption can

 doi:10.20944/preprints202602.0325.v1

be implemented either via additional sorbent cartridges or preferably integrated directly into multilayer membrane architectures incorporating activated carbon.

Such technology could be integrated into a dialysate regeneration system and may even be used in the development of portable artificial kidneys. Furthermore, innovative approaches could enable the miniaturization of hydraulic systems to achieve compact, portable dialysis units. However, it's important to recognize that improving efficiency isn't solely reliant on enhancing membrane permeability and solute clearance. Increasing treatment time and frequency also holds the potential for immediate positive outcomes, and this approach is already feasible.

References

1. Lang T, Zawada AM, Theis L, Braun J, Ottillinger B, Kopperschmidt P; et al. Hemodiafiltration: Technical and Medical Insights. Bioengineering (Basel). 2023;10(2).
2. Bowry SK, Canaud B. Achieving high convective volumes in on-line hemodiafiltration. Blood Purif. 2013;35 Suppl 1:23-8.
3. Canaud B, Barbieri C, Marcelli D, Bellocchio F, Bowry S, Mari F; et al. Optimal convection volume for improving patient outcomes in an international incident dialysis cohort treated with online hemodiafiltration. Kidney Int. 2015;88(5):1108-16.
4. Canaud B, Koehler K, Bowry S, Stuard S. What Is the Optimal Target Convective Volume in On-Line Hemodiafiltration Therapy? Contrib Nephrol. 2017;189:9-16.
5. Group ObotEW. II.2 Haemodialysis dose quantification: Middle molecules (MM). Nephrology Dialysis Transplantation. 2002;17(suppl_7):21-3.
6. Blankestijn PJ, Vernooij RWM, Hockham C, Strippoli GFM, Canaud B, Hegbrant J; et al. Effect of Hemodiafiltration or Hemodialysis on Mortality in Kidney Failure. N Engl J Med. 2023;389(8):700-9.
7. Vernooij RWM, Hockham C, Strippoli G, Green S, Hegbrant J, Davenport A; et al. Haemodiafiltration versus haemodialysis for kidney failure: An individual patient data meta-analysis of randomised controlled trials. Lancet. 2024.
8. Peters SA, Bots ML, Canaud B, Davenport A, Grooteman MP, Kircelli F; et al. Haemodiafiltration and mortality in end-stage kidney disease patients: A pooled individual participant data analysis from four randomized controlled trials. Nephrol Dial Transplant. 2016;31(6):978-84.
9. Canaud B. Recent advances in dialysis membranes. Curr Opin Nephrol Hypertens. 2021;30(6):613-22.
10. Wanner C, Vanholder R, Ortiz A, Davenport A, Canaud B, Blankestijn PJ; et al. Proceedings of a membrane update symposium: Advancements, scientific insights, and future trends for dialysis membranes for enhanced clinical outcomes in end stage kidney disease patients. Front Nephrol. 2024;4:1455260.
11. Ronco C, Clark WR. Haemodialysis membranes. Nat Rev Nephrol. 2018;14(6):394-410.
12. Canaud B, Bosc JY, Leray H, Stec F, Argiles A, Leblanc M; et al. On-line haemodiafiltration: State of the art. Nephrol Dial Transplant. 1998;13 Suppl 5:3-11.
13. Ronco C, Bowry S. Nanoscale modulation of the pore dimensions, size distribution and structure of a new polysulfone-based high-flux dialysis membrane. Int J Artif Organs. 2001;24(10):726-35.
14. Ronco C, Bowry SK, Brendolan A, Crepaldi C, Soffiati G, Fortunato A; et al. Hemodialyzer: From macro-design to membrane nanostructure; the case of the FX-class of hemodialyzers. Kidney Int Suppl. 2002(80):126-42.
15. Ronco C, Marchionna N, Brendolan A, Neri M, Lorenzin A, Martínez Rueda AJ. Expanded haemodialysis: From operational mechanism to clinical results. Nephrol Dial Transplant. 2018;33(suppl_3):iii41-iii7.
16. Kandi M, Brignardello-Petersen R, Couban R, Wu C, Nesrallah G. Effects of Medium Cut-Off Versus High-Flux Hemodialysis Membranes on Biomarkers: A Systematic Review and Meta-Analysis. Can J Kidney Health Dis. 2022;9:20543581211067090.
17. Zickler D, Schindler R, Willy K, Martus P, Pawlak M, Storr M; et al. Medium Cut-Off (MCO) Membranes Reduce Inflammation in Chronic Dialysis Patients-A Randomized Controlled Clinical Trial. *PLoS ONE*. 2017;12(1):e0169024.
18. Hornig C, Bowry SK, Kircelli F, Kendzia D, Apel C, Canaud B. Hemoincompatibility in Hemodialysis-Related Therapies and Their Health Economic Perspectives. J Clin Med. 2024;13(20).

 doi:10.20944/preprints202602.0325.v1

19. Heilmann K, Keller T. Polysulfone: The development of a membrane for convective therapies. Contrib Nephrol. 2011;175:15-26.
20. Bowry SK. Membrane requirements for high-flux and convective therapies. Contrib Nephrol. 2011;175:57-68.
21. Zawada AM, Emal K, Förster E, Saremi S, Delinski D, Theis L; et al. Hydrophilic Modification of Dialysis Membranes Sustains Middle Molecule Removal and Filtration Characteristics. Membranes (Basel). 2024;14(4).
22. Zawada AM, Melchior P, Erlenkötter A, Delinski D, Stauss-Grabo M, Kennedy JP. Polyvinylpyrrolidone in hemodialysis membranes: Impact on platelet loss during hemodialysis. Hemodial Int. 2021;25(4):498-506.
23. Maduell F, Navarro V, Hernández-Jaras J, Calvo C. [Comparison of dialyzers in on-line hemodiafiltration]. Nefrologia. 2000;20(3):269-76.
24. Werynski A, Waniewski J. Theoretical description of mass transport in medical membrane devices. Artif Organs. 1995;19(5):420-7.
25. Rangel AV, Kim JC, Kaushik M, Garzotto F, Neri M, Cruz DN; et al. Backfiltration: Past, present and future. Contrib Nephrol. 2011;175:35-45.
26. Ronco C. Backfiltration in clinical dialysis: Nature of the phenomenon, mechanisms and possible solutions. Int J Artif Organs. 1990;13(1):11-21.
27. Ronco C, Orlandini G, Brendolan A, Lupi A, La Greca G. Enhancement of convective transport by internal filtration in a modified experimental hemodialyzer: Technical note. Kidney Int. 1998;54(3):979-85.
28. Eloot S, De Wachter D, Vienken J, Pohlmeier R, Verdonck P. In vitro evaluation of the hydraulic permeability of polysulfone dialysers. Int J Artif Organs. 2002;25(3):210-6.
29. Fournier A, Birmelé B, François M, Prat L, Halimi JM. Factors associated with albumin loss in post-dilution hemodiafiltration and nutritional consequences. Int J Artif Organs. 2015;38(2):76-82.
30. Röckel A, Hertel J, Fiegel P, Abdelhamid S, Panitz N, Walb D. Permeability and secondary membrane formation of a high flux polysulfone hemofilter. Kidney Int. 1986;30(3):429-32.
31. Storr M, Ward RA. Membrane innovation: Closer to native kidneys. Nephrol Dial Transplant. 2018;33(suppl_3):iii22-iii7.
32. Starling EH. On the Absorption of Fluids from the Connective Tissue Spaces. J Physiol. 1896;19(4):312-26.
33. Nitta S, Ohnuki T, Ohkuda K, Nakada T, Staub NC. The corrected protein equation to estimate plasma colloid osmotic pressure and its development on a nomogram. Tohoku J Exp Med. 1981;135(1):43-9.
34. Landis E, Pappenheimer J. Exchange of substances through the capillary walls. In: Handbook of Physiology Circulation Washington, DC: Am Physiol Soc. 1963;II(II):961-1043.
35. Schneditz D, Sarikakis G, Kontodima M, Sauseng N. The Influence of Colloid Osmotic Pressure on Hydrostatic Pressures in High- and Low-Flux Hemodialyzers. Artif Organs. 2018;42(5):525-32.
36. Metry G, Adhikarla R, Schneditz D, Ronco C, Levin NW. Effect of changes in the intravascular volume during hemodialysis on blood viscoelasticity. Indian J Nephrol. 2011;21(2):95-100.
37. Canaud B, Bragg-Gresham JL, Marshall MR, Desmeules S, Gillespie BW, Depner T; et al. Mortality risk for patients receiving hemodiafiltration versus hemodialysis: European results from the DOPPS. Kidney Int. 2006;69(11):2087-93.
38. Grooteman MP, van den Dorpel MA, Bots ML, Penne EL, van der Weerd NC, Mazairac AH; et al. Effect of online hemodiafiltration on all-cause mortality and cardiovascular outcomes. J Am Soc Nephrol. 2012;23(6):1087-96.
39. Ok E, Asci G, Toz H, Ok ES, Kircelli F, Yilmaz M; et al. Mortality and cardiovascular events in online haemodiafiltration (OL-HDF) compared with high-flux dialysis: Results from the Turkish OL-HDF Study. Nephrol Dial Transplant. 2013;28(1):192-202.
40. Maduell F, Moreso F, Pons M, Ramos R, Mora-Macia J, Carreras J; et al. High-efficiency postdilution online hemodiafiltration reduces all-cause mortality in hemodialysis patients. J Am Soc Nephrol. 2013;24(3):487-97.
41. Davenport A, Peters SA, Bots ML, Canaud B, Grooteman MP, Asci G; et al. Higher convection volume exchange with online hemodiafiltration is associated with survival advantage for dialysis patients: The effect of adjustment for body size. Kidney Int. 2016;89(1):193-9.

 doi:10.20944/preprints202602.0325.v1

42. Gayrard N, Ficheux A, Duranton F, Guzman C, Szwarc I, Vetromile F; et al. Consequences of increasing convection onto patient care and protein removal in hemodialysis. *PLoS ONE*. 2017;12(2):e0171179.
43. Kirsch AH, Lyko R, Nilsson LG, Beck W, Amdahl M, Lechner P; et al. Performance of hemodialysis with novel medium cut-off dialyzers. Nephrol Dial Transplant. 2017;32(1):165-72.
44. García-Prieto A, Vega A, Linares T, Abad S, Macías N, Aragoncillo I; et al. Evaluation of the efficacy of a medium cut-off dialyser and comparison with other high-flux dialysers in conventional haemodialysis and online haemodiafiltration. Clin Kidney J. 2018;11(5):742-6.
45. Errill EW. Rheology of blood. Physiol Rev. 1969;49(4):863-88.
46. Canaud B, Gagel A, Peters A, Maierhofer A, Stuard S Does online high-volume hemodiafiltration offer greater efficiency and sustainability compared with high-flux hemodialysis? A detailed simulation analysis anchored in real-world data. Clinical Kidney Journal , 2024, vol. 0, no. 0, sfae147; doi.org/10.1093/ckj/sfae147.
47. Stuard, S.; Maddux, F.W.; Canaud, B.: Why High-Volume Post-Dilution Hemodiafiltration Should Be the New Standard in Dialysis Care: A Comprehensive Review of Clinical Outcomes and Mechanisms. J. Clin. Med. 2025, 14, 4860. https://doi.org/10.3390/jcm14144860.
48. Groß M; et al. The Donnan equilibrium is still valid in high-volume HDF. IJAO 2024; doi.org/10.1177/03913988241296699.
49. Zhang, Y.;Winter, A.; Ferreras, B.A.; Carioni, P.; Arkossy, O.; Anger, M.; Kossmann, R.; Usvyat, L.A.; Stuard, S.; Maddux, F.W. Real-world effectiveness of hemodialysis modalities: A retrospective cohort study. BMC Nephrol. 2025, 26, 9.
50. Strogoff-de-Matos, J.P.; Canziani, M.E.F.; Barra, A.B.L. Mortality on Hemodiafiltration Compared to High-Flux Hemodialysis: A Brazilian Cohort Study. Am. J. Kidney Dis. 2025.
51. ISO 23500 Series: Ensuring Quality of Fluids for Hemodialysis and Related Therapies; International Organization for Standardization, ISO Central Secretariat, Chemin de Blandonnet 8, CP 401, 1214 Vernier (Geneva), Switzerland.
52. Abad, S.; Vega, A.; Quiroga, B.; Arroyo, D.; Panizo, N.; Reque, J.E.; Lopez-Gomez, J.M. Protein-bound toxins: Added value in their removal with high convective volumes. Nefrologia **2016**, 36, 637–642.
53. Thammathiwat, T.; Tiranathanagul, K.; Limjariyakul, M.; Chariyavilaskul, P.; Takkavatakarn, K.; Susantitaphong, P.; Meesangnin, S.; Wittayalertpanya, S.; Praditpornsilpa, K.; Eiam-Ong, S. Super high-flux hemodialysis provides comparable effectiveness with high-volume postdilution online hemodiafiltration in removing protein-bound and middle-molecule uremic toxins: A prospective cross-over randomized controlled trial. Ther. Apher. Dial. **2021**, 25, 73–81.
54. Lima, J.D.; Guedes, M.; Rodrigues, S.D.; Florido, A.C.S.; Moreno-Amaral, A.N.; Barra, A.B.; Canziani, M.E.; Cuvello-Neto, A.; Poli-de-Figueiredo, C.E.; Pecoits-Filho, R.; et al. High-volume hemodiafiltration decreases the pre-dialysis concentrations of indoxyl sulfate and p-cresyl sulfate compared to hemodialysis: A post-hoc analysis from the HDFit randomized controlled trial. J. Nephrol. **2022**, 35, 1449–1456.
55. Hebibi H, Attaf D, Cornillac L, Achiche J, El Boundri F, Français P, Chazot C, Canaud B. Arterial Versus Venous Port Site Administration of Nadroparin for Preventing Thrombosis of Extracorporeal Blood Circuits in Patients Receiving Hemodiafiltration Treatment. Kidney International Reports. 2021;6(2):351–356. https://doi.org/10.1016/j.ekir.2020.11.020.
56. Rodriguez A, Morena M, Bargnoux A-S, Chenine L, Leray-Moragues H, Cristol J-P, Canaud B. Quantitative assessment of sodium mass removal using ionic dialysance and sodium gradient as a proxy tool: Comparison of high-flux hemodialysis versus online hemodiafiltration. Artificial Organs. 2021;45(8):E280–E292. https://doi.org/10.1111/aor.13923.
57. Ronco C, Maduell F, Kalantar-Zadeh K, Madero M, Reis T. The Role of Online Hemodiafiltration in Contemporary Kidney Care. Clin J Am Soc Nephrol. 2025 Oct 6. https://doi.org/10.2215/CJN.0000000920. Epub ahead of print. PMID: 41051878.
58. Lang T, Zawada AM, Theis L, Braun J, Ottillinger B, Kopperschmidt P, Gagel A, Kotanko P, Stauss-Grabo M, Kennedy JP, Canaud B. Hemodiafiltration: Technical and Medical Insights. Bioengineering (Basel). 2023 Jan 21;10(2):145. https://doi.org/10.3390/bioengineering10020145. PMID: 36829639; PMCID: PMC9952158.

 doi:10.20944/preprints202602.0325.v1